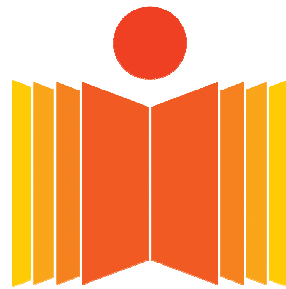


Numerical simulation of spin coating process for circular disc

SOMASHEKARA M A

A Dissertation Submitted to
Indian Institute of Technology Hyderabad
In Partial Fulfillment of the Requirements for
The Degree of Master of Technology



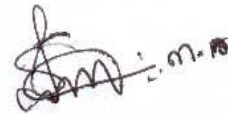
भारतीय प्रौद्योगिकी संस्थान हैदराबाद
Indian Institute of Technology Hyderabad

Department of Mechanical Engineering

July, 2011

Declaration

I declare that this written submission represents my ideas in my own words, and where others' ideas or words have been included, I have adequately cited and referenced the original sources. I also declare that I have adhered to all principles of academic honesty and integrity and have not misrepresented or fabricated or falsified any idea/data/fact/source in my submission. I understand that any violation of the above will be a cause for disciplinary action by the Institute and can also evoke penal action from the sources that have thus not been properly cited, or from whom proper permission has not been taken when needed.



(Signature)

SOMASHEKARA.M.A

(Student Name)

ME09G010

(Roll No)

Approval Sheet

This thesis entitled "Numerical simulation of spin coating process for circular disc" by Mr.SOMASHEKARA M A is approved for the degree of Master of Technology from IIT Hyderabad.



Dr.Kirti Chandra Sahu

External Examiner

Assistant Professor

Department of Chemical Engineering

IIT Hyderabad



Dr.Abhay Sharma

Internal Examiner

Assistant Professor

Department of Mechanical Engineering

IIT Hyderabad



Dr.Raja Banerjee

Adviser

Assistant Professor

Department of Mechanical Engineering

IIT Hyderabad



Dr. Saptarshi Majumdar

Chairman

Assistant Professor

Department of Chemical Engineering

IIT Hyderabad

Acknowledgements

With immense pleasure I express my deep and sincere gratitude, regards and thanks to my thesis advisor **Dr. Raja Banerjee** for his excellent guidance, invaluable suggestions and continuous encouragement at all the stages of my research work. His wide knowledge and logical way of thinking have been of great value for me. As a guide he has a great influence on me, both as a person and as a professional. Without his support I would not completed my project work.

I would like to thank Prof Desai Director of IIT Hyderabad and Prof **Vinayaka Eswaran** HOD for Department of Mechanical Engineering for approving this project and guiding, encourage me all through the course of the project.

I would like to thank Prof M.S **Ananth** Director of IIT Madras and **prof Venkateshan S P** Head of Department, Mechanical Engineering for allowing to do one semester course of my post graduate.

It was a great pleasure me as a part of Department of Mechanical IIT Hyderabad and I would like to thank all the staff members and my friends for helping me in all stages of my work and making the a great place to work in.

I would like to thank all my friends specially **M.Tech** friends for their inspiration and friendship making the life at IIT Hyderabad memorable.

I special thank my parents for their love and support while I decided to be a “professional” student for awhile.

Above all, I am blessed with such caring parents. I extend my deepest gratitude to my parents and my loving Sister **Manjula** and elder brother's **Shiva kumar, Jayachandra** and younger brother **Shiva Raj Kumar** for their invaluable love, affection, encouragement and support.

**Dedicated
To
My parents**

Abstract

The process of applying a uniform thin film on a horizontal substrate is called spin coating. Spin coating relatively used in several industrial and scientific applications. In this study an attempted was made to numerically study the various factors affecting the spin coating process.

CFD simulations were performed on 2D axisymmetric geometry, VOF multiphase model was used to its work the liquid/gas interface, results from isothermal CFD simulation were first validated against theoretical values. Subsequently, CFD simulations were performed to determine the effects of flow important parameters. Parametric study was a alone to see the effect of spin, thermo viscosity and thermo capillary on spin coating process.

Nomenclature

Symbol	Description	unit
h, h_0	Film thickness, initial	m
σ	Surface tension	N/m
ρ	Density	kg/m ³
R	Radius of disc	cm
r	Droplet radius	cm
T	Temperature	K
V_0	Dosing volume	m ³
t	time	s
u, u_R, u_θ	Liquid velocity, radial, tangential	m/s
F_c	Centrifugal force	N
η	Dynamic viscosity	kg/ms
q	Volumetric flow	m ³ /s
ω	Rotational speed	rad/s
m	Mass	kg

Contents

Declaration.....	ii
Approval Sheet	iii
Acknowledgements.....	iv
Abstract.....	vi
Nomenclature	vii
Chapter 1	1
1.1 General Principles of Coating Formulation.....	1
1.1.1 Binders.....	1
1.1.2 Pigments	2
1.1.3 Solvents.....	2
1.1.4 Additives	2
1.2 Various types of coating process	3
1.2.1 Spin coating process.....	4
1.2.2 Dip-coating.....	4
1.2.3 Flow-coating	4
1.2.4 Spray-coating.....	4
1.2.5 Thermal spray coating	5
1.2.6 Plasma polymerization	5
1.2.7 Pulsed laser deposition.....	6
1.2.8 Grafting	6
1.3 Details of spin coating process.....	8
1.3.1 Static despense.....	8
1.3.2 Dynamic despense	8
1.4 Background of spin coating process	10
1.5 Literature review	13
1.6 Motivation	17
1.3 Problem description	17
Chapter 2	
2.1 Theory of spin coating process	18

2.1.1	Liquid on Stationary disc	18
2.1.2	Liquid on rotating disc	19
2.1.3	Modeling of spin coating when liquid on rotating disc	19
2.1.4	Effects of temperature on viscosity	22
2.1.5	Effect of surface tension	24
2.2	Numerical procedure.....	25
2.2.1	The Volume of fluid flow (VOF).....	25
2.2.2	Volume Fraction Equation	26
2.2.3	The Explicit Scheme	27
2.2.4	Material properties	27
2.2.5	Momentum Equation	28
2.2.6	Energy equation	28
2.2.7	Surface Tension and Wall Adhesion.....	29

Chapter 3

3.1	Droplet on stationary disc.....	33
3.2	Validation of results	35
3.3	Droplet spreading on rotating disc	36
3.4	Droplet spreading on rotation disc for different viscosity.....	37
3.5	Simulation results for different viscosity	39
3.6	Droplet spreading on rotation disc with different rpm	42
3.7	Droplet spreading on rotating with heating the disc.....	37
3.8	Advantages of spin coating process.....	47
3.9	Disadvantages of spin coating process	48
	Figures	x
	list of tables	xi
	Conculsion	48
	Appendix	49
	list of tables	50

List of figures

1.1 Schematic of spin coating process	6
1.2 Depositing droplet on disc	7
1.3 Spin speed	9
2.1.1 Model of spin coating process	19
2.2.1 Four stages of spin coating process	20
3.1 Geometric model for spin coating process.....	31
3.2 2D mess for spin coating process.....	32
3.3 Simulation results of droplet spreading on stationary disc.....	33
3.4 X-Y plot droplet spreading on disc at different time.....	34
3.5 Film thickness when increasing time.....	34
3.6 Theoretical film thickness for different viscosity.....	38
3.7.1 Simulation results for different viscosity.....	40
3.7.2 For constant time film thickness for different viscosity.....	40
3.8 Comparing the simulation results with theoretical results.....	41
3.9 Shows the theoretical and simulation results for different rpm.....	44
3.10 For constant disc rpm and with varying the temperature of the disc rpm.....	45
3.11 For constant temperature and spin time with varying the different disc rpm.....	45

List of tables

3.1 Material properties.....	33
3.2 results of theoretical value for a different viscosity.....	37
3.3 Simulation results for different viscosity.....	39
3.4 Theoretical results for different disc rpm.....	42
3.5 Simulation results for different disc rpm.....	45
3.6 Film thickness for different temperature and disc rpm.....	45

Chapter 1

Introduction

Coating is a covering that is applied to the surface of an object, usually referred to as the substrate. In many cases coatings are applied to improve surface properties of the substrate, such as appearance, adhesion, wettability, corrosion resistance, wear resistance, and scratch resistance. In other cases, in particular in printing processes and semiconductor device fabrication (where the substrate is a wafer), the coating forms an essential part of the finished product.

Coating and printing processes involve the application of a thin film of functional material to a substrate, such as paper, fabric, film, foil or sheet stock. The coating and the process of its application is dependent on the substrate.

1.1 General Principles of Coating Formulation

Once the purpose of the coating has been identified, there are certain basic principles that can be followed to produce an effective coating. Most coatings consist of four basic ingredients, namely, a binder, pigments, solvents and additives. Some coating process may not have all of these ingredients. For example, a 100% solids plural spray epoxy contains no solvents, while an auto-motive clear coat contains no pigments. Nevertheless, it is important for the formulator to understand the roles of these basic ingredients and how they interact with one another [1].

1.1.1 Binders

A coating's binder is the 'glue' which holds it together, and which is principally responsible for providing adhesion to the substrate. With a few exceptions, the binder is nearly always organic, consisting of natural resins or

man-made polymers or pre-polymers. There are numerous types of binders for various applications such as alkyds, vinyl's, natural resins and oils, epoxies and urethanes.

1.1.2 Pigments

Pigments can affect a coating's corrosion resistance, physical properties and appearance. They are commonly grouped into two categories, namely, inorganic and organic. Inorganic pigments consist of discreet particles, often crystalline in nature, which are dispersed in paints, often with the aid of special additives which improve their compatibility with various resin systems. They can contribute to all three of the pigment functions listed above, that is, corrosion resistance, physical properties and aesthetics. Two of the most common inorganic pigments are titanium dioxide and iron oxide. Titanium dioxide is the most widely used white pigment, particularly for exterior coatings. It has a high refractive index, which means that it has excellent hiding strength, and also provides a measure of stability against the harsh ultra-violet rays of sunlight, which can degrade many coating binders. Iron oxide, of which there are many varieties, is perhaps the most common inorganic red pigment and is used in both primers and topcoats. Both synthetic and natural iron oxides exist.

1.1.3 Solvents

With very few exceptions, most coatings require solvents to dissolve the binder and to modify the viscosity so that the coating can be applied by conventional methods. Solvents evaporate after the coating has been applied and aid in the flow and leveling of the coating, as well as the wetting of the substrate. Solvents are generally thought of as organic liquids, although in a latex paint the main solvent is water.

Certain solvents can dissolve or 'cut' some resins more effectively than others. The ability of a solvent to do this is reflected in its solubility parameter, a concept that can be applied to both solvents and resins. Solubility parameters share one of organic chemistry's simplest rules,

namely, the concept of ‘like dissolves like. For instance, polar solvents are more effective than non-polar ones in dissolving polar resins.

1.1.4. Additives

Additives are various chemicals, typically added in small amounts, which can greatly affect the properties of a coating. These include surfactants, anti-settling agents, coalescing agents, anti-skinning agents, catalysts, defoamers, ultraviolet light absorbers, dispersing agents, preservatives, driers and plasticizers.

1.2. Various types of coating process

1.2.1 Spin coating process

Spin coating is a procedure used to apply uniform thin films to flat substrates. In short, an excess amount of a solution is placed on the substrate, which is then rotated at high speed in order to spread the fluid by centrifugal force. Spin coating is an important way of creating thin films in the microelectronics industry.

The controllability of the spin-coating process is excellent when it comes to creating a well-defined film with a homogeneous lateral and vertical polymer distribution. However, the spin-coating process is limited to planar substrates, which limits the applicability of the process. Other related techniques are therefore often considered. In the following various alternatives are described and compared to the spin-coating technique.

1.2.2 Dip-coating

The dip-coating technique is a crude version of the spin-coating technique. In dip coating the substrate is immersed in a polymer solution and then withdrawn. If the substrate is planar a fairly well-defined polymer film is obtained.

The film thickness can be controlled by the withdrawal velocity and by the concentration or viscosity. For non-planar substrates the controllability is lower, e.g. the film thickness will not be homogeneous.

1.2.3 Flow-coating

The flow-coating technique resembles dip-coating, but the polymer solution is poured and guided over the substrate instead of dipping the substrate into the solution. The film thickness can be controlled by the angle of inclination of the substrate and the concentration or viscosity of the polymer solution. The controllability and applicability of flow-coating is similar to that of dip-coating.

1.2.4 Spray-coating

The spray-coating technique is widely used in industrial applications. A polymer solution is sprayed creating an aerosol of the polymer solution, which is directed towards the substrate where the polymer solution is deposited. The solvent partly evaporates during spraying and the remaining solvent evaporates after deposition. Compared to dip coating the technique is very fast, but for non-planar substrates (irregularly shaped objects) the controllability of the film thickness is low. Controlling the droplet size of the aerosol can to a certain extent control the homogeneity of the polymer film. Lupoi et al. [2] studied about deposition metallic coating by using cold spray coating.

1.2.5 Thermal spray-coating

Thermal spray-coating is a solvent-free alternative to spin-coating. Polymer powder is exposed to a heat source (e.g. plasma or flame) and the resulting particles are sprayed onto a preheated substrate. The film thickness is controlled by the number of times the substrate is sprayed. The homogeneity is partly controlled by the particle size. The technique can be used on irregularly shaped objects, but the controllability is low compared to spin-coating on planar substrates.

1.2.6 Plasma polymerization

Plasma polymerization has become a widely developed and applicable technique. A monomer (typically mixed with argon) is introduced into a vacuum chamber. A field is applied between two electrodes creating plasma of chemically active species (activated molecules, radicals, ions and electrons).

The species react with each other and with the substrate of the object placed in the chamber, resulting in the formation of a plasma polymerized thin-film. The plasma polymerization product is covalently bonded to the substrate, and the cross-linking between the chains and between the chains and the substrate prevents mobilization. Controlling the experimental conditions can control the thickness and the homogeneity of the film. Plasma polymerization can be applied to planar surfaces as well as to irregularly shaped objects. However, it has the significant drawback of being a vacuum technique, which is comparatively slow and complicated for production purposes, and it is only to some extent possible to control the chemistry of the plasma-polymerized film. The inherent cross linking of the resulting polymer layer may also be incompatible with further chemical patterning processes, e.g. photo- or electron lithography.

1.2.7 Pulsed laser deposition

PLD is a solvent-free ultra-high vacuum (UHV) technique. A rotating polymer target situated in a UHV chamber is heated by a laser beam, causing evaporation of polymer particles and further absorption of laser light resulting in plasma formation and expansion. The plasma is then deposited on the substrate situated in the direction of the plasma. The drawbacks are similar to that of plasma polymerization, i.e. being a vacuum technique and having a fairly low chemical controllability due to thermal and possibly photochemical degradation products. Jürgen et al. [3] studied about industrial application from pulsed laser deposition.

1.2.8 Grafting

Polymers possessing reactive functional groups (e.g. carboxyl-terminated) can be grafted onto a substrate (e.g. a silicon surface), often via a spacer (e.g. 3 glycidoxypropyltrimethoxysilane) that chemically anchors the polymer to the substrate.⁹² It is possible to produce fairly thick polymer films (several hundreds of nanometers), which can be controlled by the molecular weight and the grafting density. For high degree of grafting and/or thick films the film will dominantly possess its intrinsic polymer properties. An

advantage of grafting is that the polymer is immobilized on the surface, a useful property in, for example, implant coatings. The fact that the coating is restricted to only a monolayer will be a disadvantage in some.

1.3 Details of spin coating process

Depositing fluid on a horizontal rotating disc produces a uniform liquid film. During deposition the disc should either be static or be rotating at a low angular velocity, where after the disc is rapidly accelerated to a high angular velocity (spin speed).

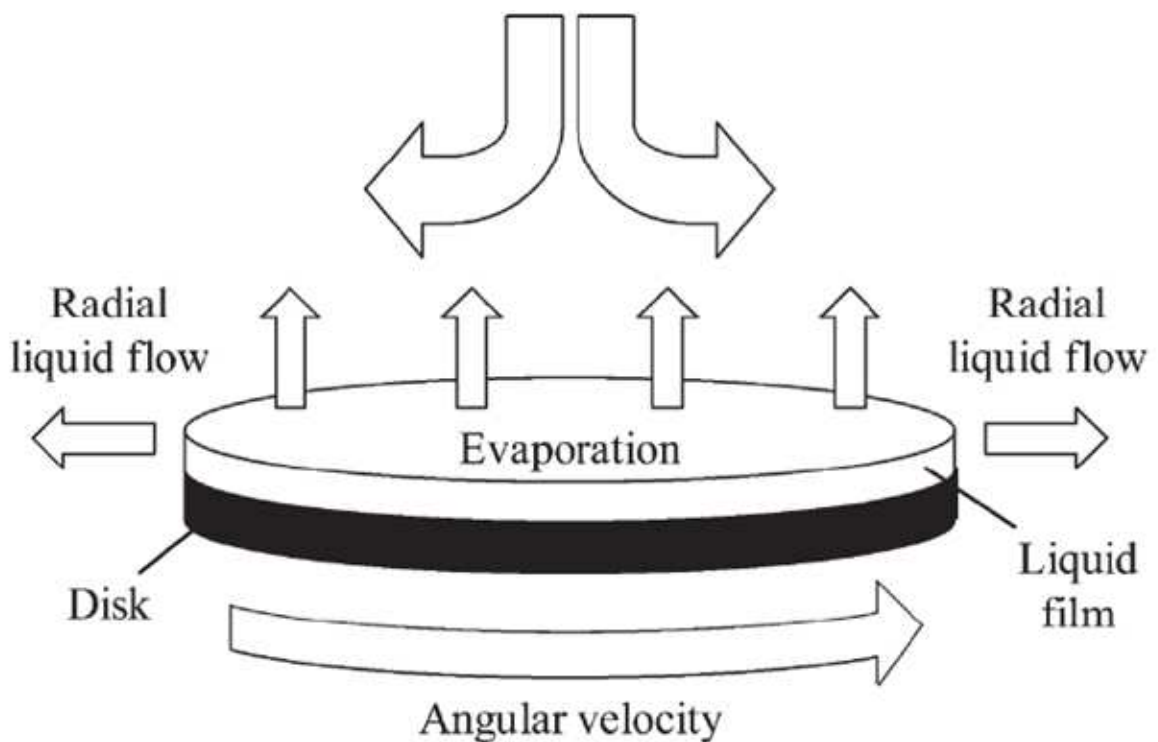


Fig1.1 Schematic of spin coating process

The adhesive forces at the liquid/substrate interface and the centrifugal forces acting on the rotating liquid result in strong sheering of the liquid which causes a radial flow in which most of the polymer solution is rapidly ejected from the disc, Fig. 1.1 This process combined with subsequent evaporation of the liquid causes the thickness of the remaining liquid film to decrease. For a solution, e.g. a polymer solution, the evaporation process causes the polymer concentration to increase (and thus the viscosity) at the

liquid/vapor interface, i.e. a concentration gradient is formed through the liquid film, which, after evaporation of most of the remaining solvent, consequently results in the formation of a uniform practically solid polymer film. Spin coating has been used for several decades for the application of thin films. A typical process involves depositing a small puddle of a fluid resin onto the center of a substrate and then spinning the substrate at high speed (typically around 3000 rpm). Centripetal acceleration will cause the resin to spread to, and eventually off, the edge of the substrate leaving a thin film of resin on the surface. Final film thickness and other properties will depend on the nature of the resin (viscosity, drying rate, percent solids, surface tension, etc.) and the parameters chosen for the spin process. Factors such as final rotational speed, acceleration, and fume exhaust contribute to how the properties of coated films are defined. One of the most important factors in spin coating is repeatability. Subtle variations in the parameters that define the spin process can result in drastic variations in the coated film. The following is an explanation of some of the effects of these variations.

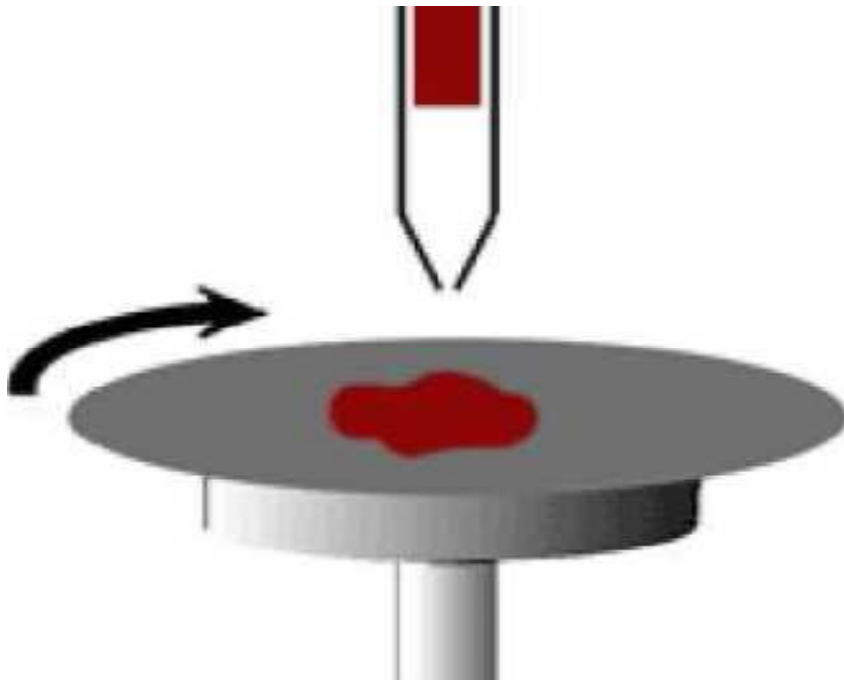


Fig 1.2 Depositing droplet on disc.

A typical spin process consists of a dispense step in which the resin fluid is deposited onto the substrate surface, a high speed spin step to thin the fluid, and a drying step to eliminate excess solvents from the resulting film. Two common methods of dispense are Static dispense, and Dynamic dispense.

1.3.1 Static dispense

Static dispense is simply depositing a small puddle of fluid on or near the center of the substrate. This can range from 1 to 10cc depending on the viscosity of the fluid and the Size of the substrate to be coated. Higher viscosity and or larger substrates typically require a larger puddle to ensure full coverage of the substrate during the high speed spin step.

1.3.2 Dynamic dispense

Dynamic dispense is the process of dispensing while the substrate is turning at low speed. A speed of about 500 rpm is commonly used during this step of the process. This serves to spread the fluid over the substrate and can result in less waste of resin material since it is usually not necessary to deposit as much to wet the entire surface of the substrate. This is a particularly advantageous method when the fluid or substrate itself has poor wetting abilities and can eliminate voids that may otherwise form. After the dispense step it is common to accelerate to a relatively high speed to thin the fluid to near its final desired thickness. Typical spin speeds for this step range from 1500-6000 rpm, again depending on the properties of the fluid as well as the substrate. This step can take from 10 seconds to several minutes. The combination of spin speed and time selected for this step will generally define the final film thickness. In general, higher spin speeds and longer spin times create thinner films. The spin coating process involves a large number of variables that tend to cancel and average out during the spin process and it is best to allow sufficient time for this to occur. A separate drying step is sometimes added after the high speed spin step to further dry the film

without substantially thinning it. This can be advantageous for thick films since long drying times may be necessary to increase the physical stability of the film before handling. Without the drying step problems can occur during handling, such as pouring off the side of the substrate when removing it from the spin bowl. In this case a moderate spin speed of about 25% of the high speed spin will generally suffice to aid in drying the film without significantly changing the film thickness. Each program on a Cree spin coater may contain up to ten separate process steps. While most spin processes require only two or three, this allows the maximum amount of flexibility for complex spin coating requirements.

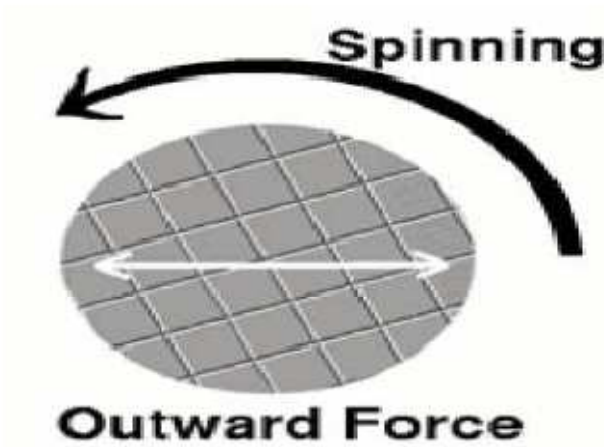


Fig3.3 Spin speed.

Spin speed is one of the most important factors in spin coating. The speed of the substrate (rpm) affects the degree of radial (centrifugal) force applied to the liquid resin as well as the velocity and characteristic turbulence, of the air immediately above it. In particular, the high speed spin step generally defines the final film thickness. Relatively minor variations of ± 50 rpm at this stage can cause a resulting thickness change of 10%. Film thickness is largely a balance between the force applied to shear the fluid resin towards the edge of the substrate and the drying rate which affects the viscosity of the resin. As the resin dries, the viscosity increases until the radial force of the spin process can no longer appreciably move the resin over the surface.

At this point, the film thickness will not decrease significantly with increased spin time. All spin coating systems are specified to be repeatable to within ± 5 rpm at all speeds. Typical performance is ± 1 rpm. Also, all programming and display of spin speed is given with a resolution of 1 rpm. Acceleration The acceleration of the substrate towards the final spin speed can also affect the coated film properties. Since the resin begins to dry during the first part of the spin cycle, it is important to accurately control acceleration. In some processes, 50% of the solvents in the resin will be lost to evaporation in the first few seconds of the process. Acceleration also plays a large role in the coat properties of patterned substrates. In many cases the substrate will retain topographical features from previous processes; it is therefore important to uniformly coat the resin over and through these features. While the spin process in general provides a radial (outward) force to the resin, it is the acceleration that provides a twisting force to the resin. This twisting aids in the dispersal of the resin around topography that might otherwise shadow portions of the substrate from the fluid.

Acceleration of spinners is programmable with a resolution of 1 rpm/second. In operation the spin motor accelerates (or decelerates) in a linear ramp to the final spin speed.

1.4 Background of spin coating process

The process of applying a solution to a horizontal rotating disc, resulting in ejection and evaporation of the solvent and leaving a liquid or solid film, is called spin coating, and has been studied and used since the beginning of the 20th century. Spin coating is a unique technique with a highly controllable and reproducible film thickness. The importance of spin-coating is manifested in its widespread use in science and industry. It is thus desirable to gain detailed understanding of the spin-coating process from both a simulation and theoretical point of view. The spin-coating technique applies to inorganic, organic and inorganic/organic solution mixtures.

Spin-coating is used in various applications such as coating of photo resist on silicon wafers, sensors, protective coatings, paint coatings, optical coatings and membranes. The most widespread use of the spin-coating technique is for microelectronics applications. Silicon is patterned using photo lithographically with a circuit design by coating semiconductor wafers with a polymeric photo resist film that is subsequently exposed through masks to transfer the circuit design. The coating of polymeric photo resist is applied by the process of spin-coating. Some of the most widely used polymers in microelectronics (and photonics) are photon or electron curable/degradable polymers (for lithographic patterning) and polyamides (e.g. for packaging, interlayer dielectrics and flexible circuit boards) [4]. For the latter applications in microelectronics, it is desirable to have low dielectric constants, good adhesion and good thermal and mechanical properties. In the area of sensors there has been much focus on spin-coating of polymer films in recent years [5-6]. For example, because of the hygroscopic properties of many polymers they have proven to be applicable in the field of relative humidity sensing, which have practical applications in the fields of medicine, meteorology, and agriculture and process control. Furthermore, the field of oxygen sensors has attracted a lot of attention [7]. The polymer is often mixed with a species that directly or indirectly produces a response and then spin-coated to produce a polymer film. The polymer normally acts as an encapsulating agent in sensor devices. The response from the sensor film is typically based on optical properties, chemistry, biological or synthetic oxygen binders, or combinations of these examples. Protective coatings are widely used in industrial applications, e.g. against corrosion, UV light, humidity and scratching Soon [8]. One of the extensive applications is spin-coating of organic dye polymers used as coatings in media for optical data mass storage [9]. A metal layer (gold, silver, copper or aluminum) is applied in order to reflect the laser light, and a thin layer of acrylic plastic is applied by spin coating for scratch protection. Finally, an extra protective or printer-friendly coating is then applied by spin-coating. One of the first applications

of spin-coating was the application of paint coatings to various industrial products. However; this process was/is limited to products with planar surfaces. A paint coating is often not just cosmetic, but also acts as a protective coating. The area of optical coatings is versatile and contains many applications where spin coating plays an important role [10]. Optical coatings with low-refractive indices are used in anti-reflection applications to improve light transmission in industrial and scientific instruments as well as in everyday optical applications. There is still much interest in optimizing broadband antireflection coatings, but the progress is hindered by the lack of materials with sufficiently low refractive indices. In recent years, fluorine-containing polymers with refractive indices approaching that of water and also suitable for spin-coating has become commercially available but their wider application awaits reduction in material costs. Spin-coated polymer films that function as membranes have applications in the above mentioned sensor applications, where the polymer film acts as an encapsulating agent and as a barrier layer [11-13]. Ion-exchange membranes are also used as sensors through their engineered contents of ionic functional groups, which can react and/or be coupled with analyses, resulting in a membrane response. Polymer membranes can also be manufactured from a micro sphere suspension in a solution of polymer, which is then spin-coated (or more commonly molded) and subsequently polymerized or cross-linked to form a hydrogel. Porous polymer membranes can be formed by spin-coating incompatible polymer blends that will phase-separate during the drying process. [14] A porous polymer film results from the selective dissolution of one of the polymers. The ability to form ever-smaller, mono disperse pores has widened the applications to even more advanced applications, such as separation of enantiomers or bimolecular, drug delivery and catalysis.

1.6 Literature review

Spin coating is one of the fundamental micro/nano fabrication methods widely employed in the fabrication of diverse microelectronic devices such as micro sensors and other MEMS devices. In spin coating, a liquid droplet placed at the origin of a rotating disk spreads outwards driven by the centrifugal spinning and eventually a thin film of uniform thickness is left on the substrate surface. Reznik, et al. [15] studied about spreading of a drop on dry plane horizontal wall under the action of gravity and surface tension in the inertialess approximation for different Bond numbers. However the initial spreading of fluid was completely dominated by gravity and rolling motion setting at different contact of line. Wetting plays an important role when the contact line motion reduces to the characteristic wetting velocity as expected from Hoffman's well-known law [16].

Bartashevich et al. [17] studied both analysis and numerically drop spreading on horizontal surface under action of gravity force at zero tangential force. Droplet analytical profile was solved using energy and Navier–Stokes equations and effects of surface tension and thermocapillarity were considered. Shape of the droplet was completely regulated by the balance between capillary forces and gravity action and drop volume was constant. Drop geometrical profile of a quarter of axisymmetric was calculated based on solution of Laplace equation.

Siddhartha et al. [18] studied drop impact and spreading on horizontal and inclined surface. The numerical simulation of the dynamics of droplet impact and spreading was carried out by using volume of fluid (VOF) method. The important factors which govern the drop dynamics on a solid surface are the liquid properties like density, surface tension and viscosity and the surface characteristics like contact angle and roughness. The influence of surface wetting characteristics was investigated by using static contact angle (SCA) and dynamic contact angle (DCA) models. It was found that when static contact angle (SCA) $> 90^\circ$ then there was less wetting and if $SCA < 90^\circ$ then there was more wetting surface. The DCA observed at

initial contact times were order of magnitude higher than SCA values and therefore the DCA model is needed for the accurate prediction of the spreading behavior.

Maxime [18] explained the spreading of a drop of neutrally buoyant suspension by the spreading of suspension drops on a flat surface was studied using mixtures of liquid and density matched particles. From the energy balance model it was shown that the spreading, the spreading factor is reduced with increasing particle volume fraction. This decrease was quantitatively understood through an effective viscosity co-efficient. However, for large drop-Reynolds number, the particles were not uniformly distributed into the spread drop but form an annulus. For higher impact velocities, a particle-induced break-up of the drop was observed.

Niranjan [19] derived mathematical model for film formation to explain the spin coating process for both Newtonian and Non-Newtonian fluids. Myers et al. [20] studied the importance of the Coriolis force on axisymmetric horizontal rotating disc using Lubrication theory. The model provides a simple relation between fluid flux and the film height. The correction terms, caused by the Coriolis force and inertia terms, lead to slightly higher predictions for the film height.

Liang et al. [22] studied polymer concentration, shear and stretch field effects on the surface morphology evolution of three different kinds of polymers polystyrene(PB), polybutadiene(PB) and polystyrene-b-polybutadiene-b-polystyrene(SBS) during the spin-coating by means of atomic force microscopy (AFM). These different transitions of surface morphologies were discussed in terms of individual material property. They investigated the polymer concentration effect on the surface morphology evolution of three different kinds of polymers (PS, PB and SBS) after spin coating. Thereafter, they compared the evolution of surface topographies of these different kinds of polymers at different locations of substrates from the center of mica flake to the edge.

YIH-O et al. [20] studied the evolution of the free surface and the slippage of the contact line. Contact line is described by a phenomenological model in which the slip coefficient is inversely proportional to the liquid film thickness. The slip rate at the contact line is given analytically in terms of the material and physical parameters that effect the slippage. Their result indicates the way toward control of slippage at the contact line.

Yimsiri et al. [21] studied experiment analysis on spin and dip coating process for light-emitting polymer (LEP) solutions. Both process were carried out but in terms of spin coating, which is a typical process for the manufacture of polymer light-emitting diodes, a number of process variables including spin speed were systematically explored.

Temple-Boyer et al. [22] studied about spin coating processes for the deposition of polysiloxane-based Maxwellian liquids by adapting hydrodynamic laws theory. Piotr et al. [23] have used spin coating process for fabrication of electrolyte layers for SOFCs and high temperature protective coatings of stainless steel, and its helps in eliminating problems related to excessive steel corrosion of metal supported SOFCs and avoid reaction between electrolyte and cathode during high temperature sintering process.

Lin et al. [24] have studied about spin coating process when the rotating disc is axisymmetrically heated and predicated effects of thin liquid film dynamics, considering both temperature dependent viscosity and temperature dependent surface tension. A nonlinear scalar equation for the film thickness profile evolution is derived under lubrication assumptions. They predicted that both thermocapillarity (temperature dependent viscosity) and thermoviscosity(temperature dependent surface tension) effects can be harnessed to enhance the liquid films depletion during spin coating. Thermoviscosity effect is important and dominates the external air shearing effect when the film thickness is relatively large. When the liquid film is thin enough, thermocapillarity effect starts to dominate centrifugal force, external air shearing and thermoviscosity effects. They used

lubrication and axisymmetric conditions, for a Newtonian flow on a rotating disk. Konstantin et al. [25] studied spin coating process of Sol-Gel Silicate films deposition mainly; two important factors that affect spin coating process of sol gel film were studied: spin speed and temperature during film deposition. A catch cup is used to collect the scattered photo resist material that is deposited during the spin coating process; this excess photo resist material is reduced from wafer edge by an exhaust flow. The boundary layer flow on the wafer surface is affected by this exhaust flow and catch cup geometry Mizue et al. [26] used Doppler velocimeter to determine the development of 3D boundary layer and optimized the design of the catch cup this James et al. [Sangjun et al. [27] developed process using extrusion spin coating process that helps reduce photoresist waste and improve coating uniformity in microlithography. This coating technique applies a thin film of resist to a wafer prior to spinning

1.6 Motivation

The spin coating process used to deposit photo resist onto wafers is one of the most mature processes in modern semiconductor manufacturing. As the industry advances to smaller devices, the depth of focus budgets for lithography processes require increasingly uniform photo resist layers. Nearly all of the research which has gone into understanding the spin coating process has been conducted using round wafers and only one reference has been found which concentrates on circular substrates. This report discusses issues associated with spin coating circular substrates in addition to theoretical techniques used to optimize the spin coating recipe and equipment set up for increasing coating uniformity. Applications using circular substrates include flat panel displays as well as products in which processing equipment constrains the substrate to circular dimensions. Although device sizes for these products are much larger than those used in semiconductor products, the progression to smaller devices for increased resolution continues. Although advanced photo resist coating techniques such

as dip coating and spray coating exist for odd shaped substrates, none have the maturity, ease of implementation, equipment simplicity, and robustness that spin coating offers.

1.7 Problem description

This project presents optimal spin coating techniques for achieving maximum photo resist uniformity over circular substrates and how these techniques influence coating thicknesses.

Simulated two problem using fluent

Problem 1. Circular substrates stationary and depositing the droplet on circular disc due to gravity and capillary action on droplet will spread over the circular substrate. Based on viscosity of fluid and temperature of disc liquid will spread over the substrate.

Problem 2. First deposit droplet on circular substrate and will give 100 rpm to circular disc due centrifugal force droplet start to deposit on disc.

Problem 3. Considering thermocapillarity (temperature dependent viscosity) and thermoviscosity (temperature dependent surface tension) effects on film thickness.

Chapter 2

Theory and numerical procedure for spin coating process

2.1 Theory of spin coating process

2.1.1 Liquid on Stationary disc

Stationary disc also called static dispense in which small puddle of fluid is placed on or near the center of the substrate. The puddle size range depends on the viscosity of the fluid and the size of the substrate to be coated. Higher viscosity and or larger substrates typically require a larger puddle to ensure full coverage of the substrate during the high speed spin step. A wall on side of the disc so, that it can prevent the droplet splash from the disc. Drop let is spreads on the disc by action of gravity and surface tension.

In the absence of shear at the gas–liquid interface and other external forces the liquid drop rounds up to minimize its surface energy. However due to gravity it flattens on the plate.

Consider the spreading axisymmetric droplet with the following assumptions:

1. The axisymmetric drop spreading on a smooth chemically homogeneous horizontal solid surface normal to the gravity.
2. The drop is surrounded by an inviscid gas (no shear at the gas–liquid interface).
3. The shape of sessile drop is regulated by the balance between capillary forces and gravity action.
4. The drop volume is constant (non-evaporating process).
5. The contact angle between the liquid and the solid surface is assumed equal to its equilibrium value.

A spherical droplet is compressed by the gravity.

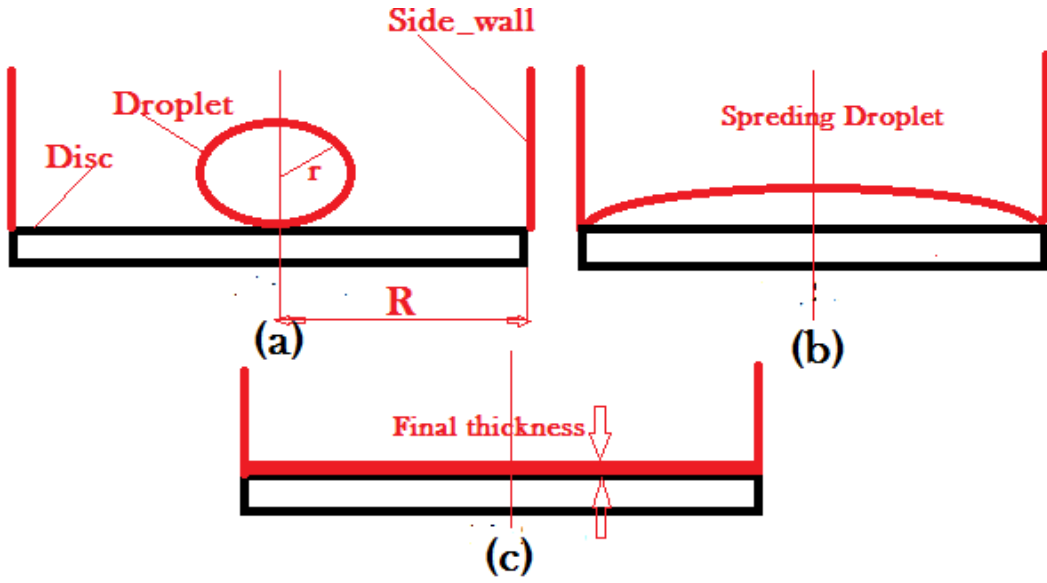


Fig 2.1.1 Schematic model of spin coating process

Fig (a) shows the initial stage of radius droplet r and R is radius of disc. Fig (b) spreading droplet and fig (c) final shape of droplet

$$\text{Volume of Droplet} = \frac{4 \pi r^3}{3} \quad (2.1)$$

$$\text{Volume of fluid on Disc} = \pi R^2 h \quad (2.2)$$

Where r = radius of droplet in cm.

R = Radius of the disc in cm.

h = thickness of coating film in cm.

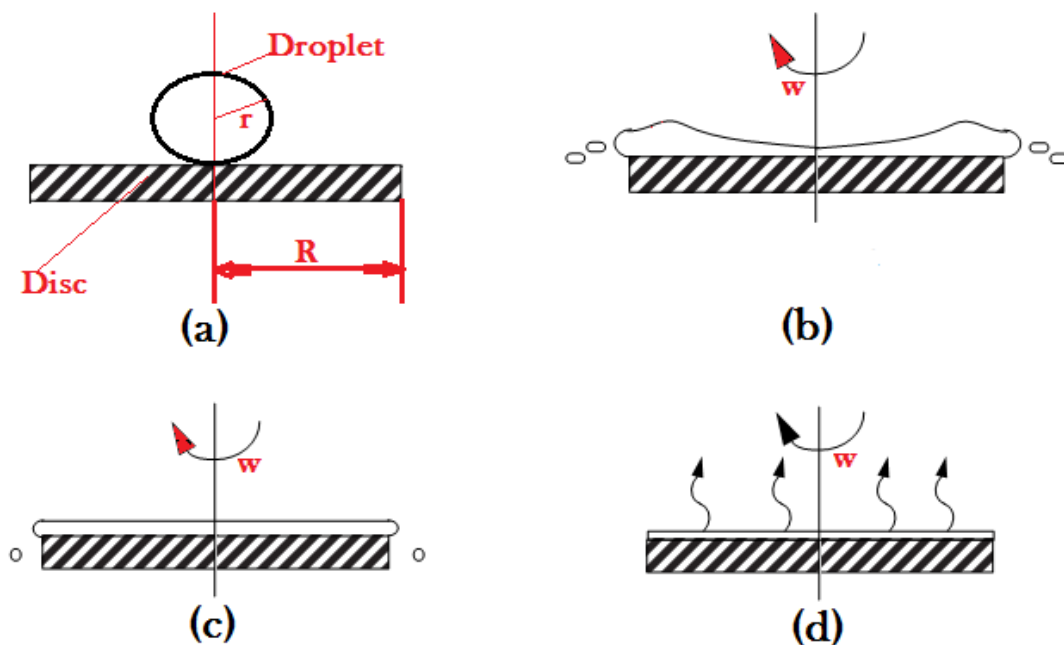
For static volume of fluid spreading on disc is equal to volume of droplet at initial stage.

$$\pi R^2 h = \frac{4 \pi r^3}{3} \quad (2.3)$$

$$\text{Film thickness } h = \frac{4}{3} \left[\frac{r}{R} \right]^2 r \quad (2.4)$$

2.1.2 Liquid on rotating disc

Spin coating is a process where a drop of liquid is placed on a substrate and spread by centrifugal force. The spin coating process can be broken down into the four stages shown in Figures 2.2. The deposition, spin up with ω , and spin off stages occur sequentially while the evaporation stage occurs throughout the process, becoming the primary means of thinning near the end.



Figures 2.1.2 four Stages of the Spin Coating Process.

Fig (a) Deposition of droplet at initial, fig (b) Spin up with ω speed, fig (c) spin off and fig (d) final stage film thickness and evaporation.

The deposition process involves the spreading of the fluid onto a spinning substrate. The fluid is deposited through a nozzle at the center of the substrate or over some programmed path. An excessive amount of fluid is used to prevent coating discontinuities caused by the fluid front drying prior to it reaching the wafer edge.

In the spin up stage, the substrate is accelerated to the final spin speed. As rotational forces are transferred upward through the fluid, a wave front forms and flows to the substrate edge by centrifugal force, leaving a fairly uniform layer of photo resist behind.

The spin off stage is the spin coating stage where the excess solvent is flung off the substrate surface as it rotates at speeds between 600 and 800 RPMs. The fluid is being thinned primarily by centrifugal forces until enough solvent has been removed to increase viscosity to a level where flow ceases.

Evaporation becomes the primary method of film thinning once fluid flow ceases. A variety of film thicknesses can be deposited by spin coating, due to film thickness being roughly inversely proportional to the square root of spin speed. As coating thicknesses increase, it becomes harder to find a solvent/solute mixture which will not dry before reaching the substrate edge. For this reason, thick films are occasionally formed by spinning on multiple thinner, more reliable coatings.

2.1.3 Modeling of spin coating when liquid on rotating disc

The relevant parameters in spin coating process are fluid properties: density ρ viscosity η and surface tension γ and spin coating process parameters dosing volume V_0 , rotation speed ω , the liquid height h , liquid radius r , the elapsed time t , disc radius R and the (dynamic) contact angle θ_D . When a drop of liquid has a cylindrical shape and evaporation is neglected, liquid height, radius and initial volume are coupled:

$$h = \frac{V_0}{\pi R^2} \quad (2.4)$$

Show a simple derivation of the equations that govern the spin coating process. A situation is considered with a stationary liquid flow on a rotating plane. The following assumptions are made:

1. The plane is horizontal, so that there is no radial gravitational component.

2. The liquid layer is radially symmetric.
3. The viscosity is independent of the rate of shear, i.e., the liquid is Newtonian.
4. The liquid layer is everywhere so thin that shear resistance is appreciable only in horizontal planes.
5. The evaporation of the liquid is negligible.

Now we take cylindrical polar coordinates $(\mathbf{r}, \boldsymbol{\theta}, \mathbf{z})$ rotating with the spinning disk at angular velocity $\boldsymbol{\omega}_R$. The z dependence of the radial velocity \boldsymbol{v}_R of the liquid at any point $(\mathbf{r}, \boldsymbol{\theta}, \mathbf{z})$ can be found by balancing the viscous and the centrifugal forces per unit volume, the centrifugal force working in the radial direction and the viscous shear stress in the opposite direction Refer to Appendix:

$$-\eta \frac{\partial^2 v_R}{\partial z^2} = \rho \omega^2 r \quad (2.5)$$

$$\text{Final film thickness } h = \frac{h_0}{\left(1 + \frac{4 \rho \omega^2 h_0^2 t}{3 \eta}\right)^{\frac{1}{2}}}, \quad (2.6)$$

Where h_0 is the initial height of droplet, t is spin time, Refer to Appendix:

2.1.4 Effects of temperature on viscosity

The viscosity of liquids decreases with increase in temperature either under isobaric conditions or as saturated liquids. This behavior can be seen john [56] where, for example, the viscosity of saturated liquid benzene is graphed as a function of temperature. Also, as noted and illustrated in fig, for a temperature range from the freezing point to somewhere around the normal boiling temperature it is often a good approximation to assume $\ln \eta_L$ is linear in reciprocal absolute temperature;

$$\ln \eta_L = A + \frac{B}{T} \quad (2.7)$$

This simple form was apparently first proposed by de Guzman John [56] (O’Loane, 1979), but it is more commonly referred to as the Andrade equation (1930, 1934). Variation of eq(7.1) John [56] have been proposed to improve upon its correction accuracy: many include some function of the liquid molar volume in either the A or B parameter (Bingham and Stookey,1939; Cornelissen and Waterman, 1955; Eversteijn, et., 1960; Girifalco, 1955; Gutman and Simmons, 1952;Innes, 1956;Marschalko and Barna, 1957; Medani and Hasan, 1977; Miller, 1963a; Telang, 1945; and van Wyk, et al., 1940). Another variation involves the use of a third constant to obtain the Vogel equation (1921),

$$\ln \eta_L = A + \frac{B}{T + C} \quad (2.8)$$

Goletz and Tassios (1977) have used this form (for the kinematic viscosity) and report values of A, B, And C for many pure liquids.

Equation (2.7) requires at least two viscosity-temperature datum points to ways to extrapolate this value is to employ the approximate Lewis-Squires chart (1934), which is based on the empirical fact that the sensitivity of viscosity to temperature variations appears to depend primarily upon the value of the viscosity. This chart shown in John [56] can be used by locating the known value of viscosity on the ordinate and then extending the abscissa by the required number of degrees to find the new viscosity, can be expressed in an equation form as

$$\eta_L^{-0.2661} = \eta_K^{-0.2661} + \frac{T - T_K}{233} \quad (2.9)$$

Where η_L = liquid viscosity at T , cP

η_K =known value of liquid viscosity at T_K , cP

T and T_K may be expressed in either $^{\circ}\text{C}$ or K . Thus, given a value of η_L at T_K , one can estimate value of η_L at other temperatures, expressed. This method should not be used if the temperature is much above the normal boiling point.

2.1.5 Effect of surface tension

Surface tension arises as a result of attractive forces between molecules in a fluid. Consider an air bubble in water, for example. Within the bubble, the net force on a molecule due to its neighbors is zero. At the surface, however, the net force is radially inward and the combined effect of the radial components of force across the entire spherical surface is to make the surface contract, thereby increasing the pressure on the concave side of the surface. The surface tension is a force, acting only at the surface that is required to maintain equilibrium in such instances. It acts to balance the radially inward inter molecular attractive force with the radially outward pressure gradient force across the surface. In regions where two fluids are separated, but one of them is not in the form of spherical bubbles, the surface tension acts to minimize free energy by decreasing the area of the interface.

The surface tension of water is temperature dependent. It decreases as temperature rises by following relationship (Stelczer, 1987):

$$\sigma = 0.0755 - 0.0001569 * T \quad (2.10)$$

Where σ =surface tension in N/m

T =Temperature in K

2.2 Numerical procedure

Model is pressure based solver with axisymmetric and unsteady state condition. Selected volume of fluid multiphase model , material select air and viscosity $1.789e-5\text{kg/m}_s$ and water density 1000kg/m^3 viscosity $0.001\text{m}^3/\text{kg}$, phase selection primary phase air and secondary phase water .

2.2.1 The Volume of fluid flow (VOF) method

The VOF formulation in fluent is generally used to compute a time-dependent solution, but for problems in which you are concerned only with a steady-state solution, it is possible to perform a steady-state calculation. A steady-state VOF calculation is sensible only when your solution is independent of the initial conditions and there are distinct in flow boundaries for the individual phases. For example, since the shape of the free surface inside a rotating cup depends on the initial level of the fluid, such a problem must be solved using the time-dependent formulation. On the other hand, the flow of water in a channel with a region of air on top and a separate air inlet can be solved with the steady state formulation.

The VOF formulation relies on the fact that two or more fluids (or phases) are not interpenetrating. For each additional phase that you add to your model, a variable is introduced: the volume fraction of the phase in the computational cell. In each control volume, the volume fractions of all phases sum to unity. The fields for all variables and properties are shared by the phases and represent volume-averaged values, as long as the volume fraction of each of the phases is known at each location. Thus the variables and properties in any given cell are either purely representative of one of the phases, or representative of a mixture of the phases, depending upon the volume fraction values.

In a computational domain under consideration, the particular fluid phase is defined by the volume fraction (α_q) in a control volume as the fraction of the q^{th} phase inside a cell as

Where

$$\alpha_q = \begin{cases} 0 & \text{If the cell is empty (of } q^{\text{th}} \text{ phase)} \\ 1 & \text{If the cell is full (of } q^{\text{th}} \text{ phase)} \end{cases} \quad (2.11)$$

If $0 < \alpha_q < 1$ the cell contains the interface between the q^{th} phase and the other phase (s). Depending upon local values of volume fraction, the appropriate properties and variables will be assigned to each control volume within the domain.

2.2.2 Volume Fraction Equation

The tracking of the interface(s) between the phases is accomplished by the solution of a continuity equation for the volume fraction of one (or more) of the phases. For the q^{th} phase, this equation has the following form:

$$\frac{1}{\rho_q} \left[\frac{\partial}{\partial t} (\alpha_q \rho_q) + \nabla \cdot (\alpha_q \rho_q \vec{v}) \right] = S_{\alpha_q} + \sum_{p=1}^n (\dot{m}_{pq} - \dot{m}_{qp}) \quad (2.12)$$

Where \dot{m}^{qp} is the mass transfer from phase q to phase p and \dot{m}_{pq} is the mass transfer from phase p to phase q. By default, the source term on the right-hand side of Equation 3.2 S_{α_q} , is zero, but you can specify a constant or user-defined mass source for each phase.

In the VOF model, the motion of a moving interface is computed by solving an advection equation for the volume fraction of the q^{th} phase (secondary-phase):

$$\frac{\partial \alpha_q}{\partial t} + \vec{v} \cdot \nabla \alpha_q = 0. \quad (2.13)$$

The volume fraction equation will not be solved for the primary phase; the primary-phase volume fraction will be computed based on the following constraint:

$$\sum_{q=1}^n \alpha_q = 1. \quad (2.14)$$

The volume fraction equation may be solved either through implicit or explicit time discretization.

2.2.3 The Explicit Scheme

In the explicit approach, fluent standard finite-difference interpolation schemes are applied to the volume fraction values that were computed at the previous time step.

$$\frac{\alpha_q^{n+1} \rho_q^{n+1} - \alpha_q^n \rho_q^n}{\Delta t} V + \sum_f (\rho_q U_f^n \alpha_{q,f}^n) = \left[\sum_{p=1}^n (\dot{m}_{pq} - \dot{m}_{qp}) + S_{\alpha q} \right] V \quad (2.15)$$

Where $n + 1 =$ index for new (current) time step

$n =$ index for previous time step

$\alpha_{q,f} =$ face value of the q th volume fraction, computed from the
First-order or Second-order upwind scheme

$V =$ volume of cell

$U_f =$ volume flux through the face, based on normal velocity

This formulation does not require iterative solution of the transport equation during each time step, as is needed for the implicit scheme.

2.2.4 Material properties

The properties appearing in the transport equations are determined by the presence of the component phases in each control volume. In a two-phase system, for example, if the phases are represented by the subscripts 1 and 2, and if the volume fraction of the second of these is being tracked, the density in each cell is given by

$$\rho = \alpha_2 \rho_2 + (1 - \alpha_2) \rho_1, \quad (2.16)$$

In general, for an n -phase system, the volume-fraction-averaged density takes on the following form:

$$\rho = \sum \alpha_q \rho_q \quad (2.17)$$

For viscosity

$$\mu = \alpha_2 \mu_2 + (1 - \alpha_2) \mu_1, \quad (2.18)$$

In general, for an n-phase system, the volume-fraction-averaged viscosity takes on the following form:

$$\mu = \sum \alpha_q \mu_q \quad (2.19)$$

2.2.5 Momentum Equation

A single momentum equation is solved throughout the domain, and the resulting velocity field is shared among the phases. The momentum equation, shown below,

$$\frac{\partial}{\partial t} (\rho \vec{v}) + \nabla \cdot (\rho \vec{v} \vec{v}) = -\nabla P + \nabla \cdot [\mu (\nabla \vec{v} + (\nabla \vec{v})^T)] + \rho \vec{g} + F, \quad (2.20)$$

Where \vec{v} is velocity vector, P is pressure, F is surface tension force per unit volume, \vec{g} is the gravitational acceleration, ρ is the density and μ is the viscosity. Depending upon volume fraction values the flow variables and the fluid properties in any given cell are either purely representative of one of the phases, or representative of a mixture of the phases. Based on the local value of α_q , the appropriate fluid properties and flow variables were assigned to each control volume within the domain eq 2.11, 2.16 2.17.

2.2.6 Energy equation

The energy equation, also shared among the phases, is shown below.

$$\frac{\partial}{\partial t} (\rho E) + \nabla \cdot (\vec{v} (\rho E + p)) = \nabla \cdot (k_{eff} \nabla T) + S_h \quad (2.21)$$

The VOF model treats energy, E , and temperature, T , as mass-averaged variables:

$$E = \frac{\sum_{q=1}^n \alpha_q \rho_q E_q}{\sum_{q=1}^n \alpha_q \rho_q} \quad (2.22)$$

As with the velocity field, the accuracy of the temperature near the interface is limited in cases where large temperature difference's exist between the phases. Such problems also arise in cases where the properties vary by several orders of magnitude. For example, if a model includes liquid metal in combination with air, the conductivities of the materials can differ by as much as four orders of magnitude. Such large discrepancies in properties lead to equation sets with anisotropic coefficients, which in turn can lead to convergence and precision limitations.

2.2.7 Surface Tension and Wall Adhesion

The VOF model can also include the effects of surface tension along the interface between each pair of phases. The model can be augmented by the additional specification of the contact angles between the phases and the walls. Specify a surface tension coefficient as a constant, and function of temperature, or through a UDF.

The surface tension model in fluent is the continuum surface force (CSF) model proposed by Brackbill et al. [34]. With this model, the addition of surface tension to the VOF calculation results in a source term in the momentum equation. It can be shown that the pressure drop across the surface depends upon the surface tension Coefficient, σ , and the surface curvature as measured by two radii in orthogonal directions,

R1 and R2:

$$p_2 - p_1 = \sigma \left(\frac{1}{R_1} + \frac{1}{R_2} \right) \quad (2.23)$$

Where p_1 and p_2 are the pressures in the two fluids on either side of the interface.

In fluent, a formulation of the CSF model is used, where the surface curvature is computed from local gradients in the surface normal at the interface. Let n be the surface normal, defined as the gradient of α_q , the volume fraction of the q^{th} phase.

$$n = \nabla \alpha_q \quad (2.24)$$

The curvature, k , is defined in terms of the divergence of the unit normal, \hat{n}

$$k = \nabla \cdot \hat{n} \quad (2.25)$$

Where

$$\hat{n} = \frac{n}{|n|} \quad (2.26)$$

The surface tension can be written in terms of the pressure jump across the surface. The force at the surface can be expressed as a volume force using the divergence theorem. It is this volume force that is the source term which is added to the momentum equation.

It has the following form:

$$F_{vol} = \sum_{pairs\ i,j, i < j} \sigma_{ij} \frac{\alpha_i \rho_i k_j \nabla \alpha_j + \alpha_j \rho_j k_i \nabla \alpha_i}{\frac{1}{2}(\rho_i + \rho_j)} \quad (2.27)$$

This expression allows for a smooth superposition of forces near cells where more than two phases are present. If only two phases are present in a cell, then $k_i = -k_j$ and $\nabla_{\alpha_i} = -\nabla_{\alpha_j}$, and Equation 2-27 simplifies to

$$F_{vol} = \sigma_{ij} \frac{\rho k_i \nabla \alpha_i}{\frac{1}{2}(\rho_i + \rho_j)} \quad (2.28)$$

Where ρ is the volume-averaged density computed using Equation 3.6. Equation 3.18 shows that the surface tension source term for a cell is proportional to the average density in the cell.

Chapter

Results and discussion

To obtain an accurate solution for spin coating process, mesh density should be such that it captures the fluid flow in the domain accurately. However, geometry with very high mesh density results in high computational time.

Geometry

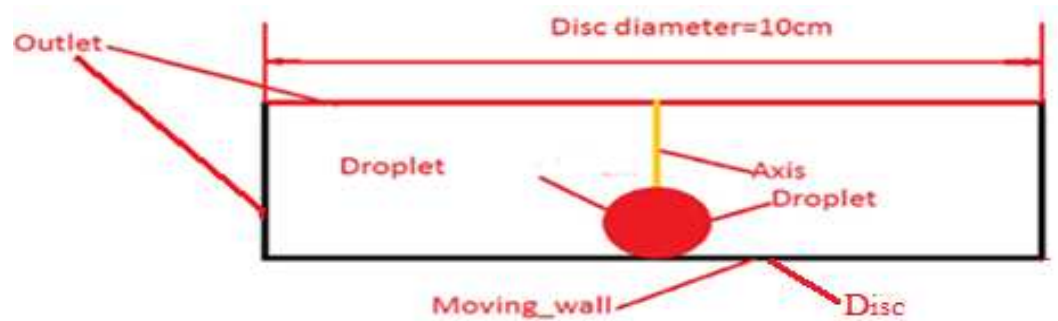


Figure 3.1 geometric model for spin coating process,

Figure 3.1.1 shows the geometric model of spin coating process, the diameter of disc is 10cm and a droplet of 1cm is placed exactly at the center of circular disc. The disc is completely open to atmosphere and is horizontally placed. Excess of fluid falls off. Spreading of the droplet on a horizontal disc is completely dominated by gravitational force when the disc is stationary. For solving this 2D mesh is created using the commercial software Hyper works. Mesh distribution should be such way that it captures the liquid/gas interface accordingly. Therefore the mesh was kept very fine near the disc surface and at the center of disc. There the region where most the deformation of the liquid/gas interface is expected to occur. The meshed fluid domain is shown, the disc is open to atmosphere, therefore atmosphere pressure boundary condition was applied to the vertical side and

the top side of the fluid domain, wall boundary condition is applied at bottom surface.

Numerical simulations were carried out using two-dimensional rectangular mesh. The extents of the solution domain X and Z-direction were decided based on drop diameter, liquid properties and surface wettability data. Typically, the solution domain for simulation of the 0.5 cm radius water depositing on horizontal surface was 2.5cm axis height 5cm long. The no slip boundary condition was specified at the wall (bottom face) and all the remaining faces were defined as the pressure outlet (as shown in Fig. 4.1.2). The user defined functions are used to implement the temperature dependence viscosity and temperature dependence of surface tension. Selected pressure based solver, absolute velocity formulation, axisymmetric, transient condition, and model is multiphase, water and air used as material table 3.1 shows properties of the water and air. Droplet is patching at the middle of axis point and model droplet shown in figure 3.1.

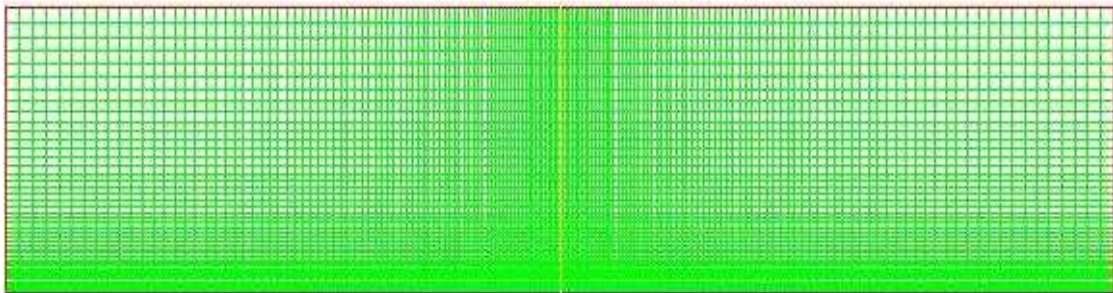


Fig3.2 2d mess for spin coating process

3.1 Droplet on stationary disc

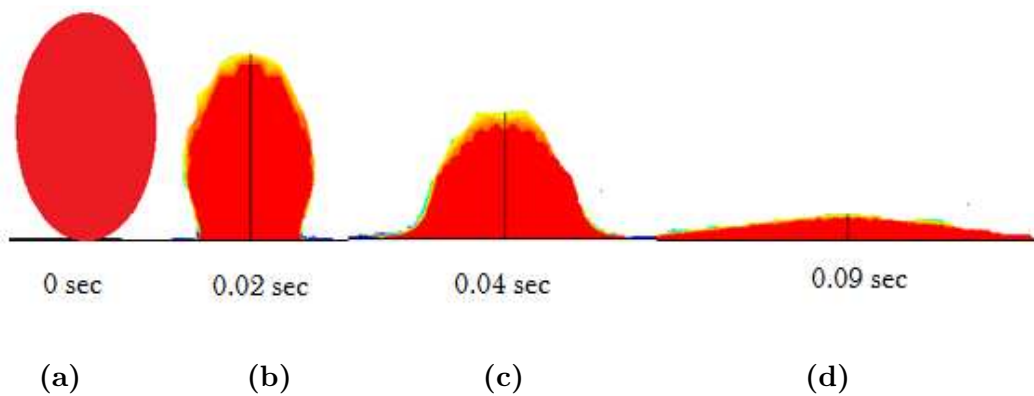


Fig 3.3 Simulation results of droplet spreading on stationary disc

Figures 4.1.3 shows simulation results of a droplet spreading on horizontal disc, droplet spreading on stationary horizontal disc was completely dominated by gravity and surface tension. Based on viscosity and density of droplet, also horizontal disc surface spreading take place. Here water as droplet figure 4.1.3(a) shows the initial size of droplet and patching at the middle of the disc 0 sec, figure 4.1.3 (b) shows the droplet compressed due gravity and surface tension after 0.02 sec, figure 4.1.3 (c) shows the droplet compressing more compare to previous one this droplet shape after 0.04 sec and after 0.09 sec figure (d), after certain second droplet completely spreads on horizontal disc based on the density and viscosity of the fluid the thickness variation on surface. I had simulated different viscosity of fluid, when the viscosity will be more spreading takes place slowly and when the viscosity of droplet is less spreading will takes very fast.

Material properties

Name fluid	Density in kg/ m ³	Viscosity in kg/m s	Specific heat in j/kg-k	Thermal conductivity in w/m-k
Water	1000	1E-3	4128	0.6
Air	1.225	1.789E-5	1006.43	0.0242

Table 3.1 Material properties

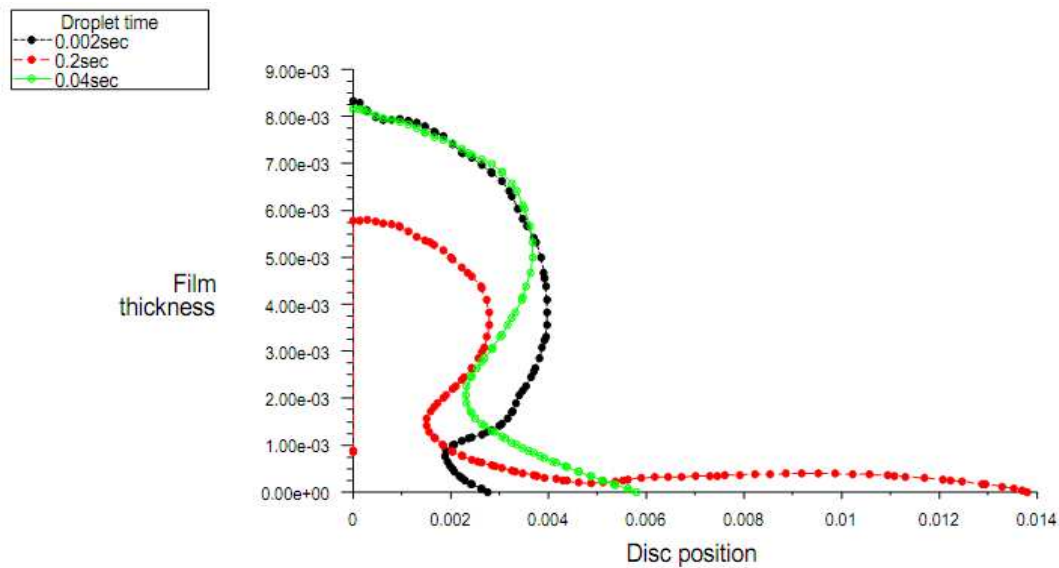


Fig 3.4 X-Y plot droplet spreading on disc at different time

Figure 4.1.4 shows the droplet spreading on horizontal disc with different time previous section discussed about how the droplet formation takes place figure show discontinuous line shows droplet spreading after time interval 0.2 sec. dark and continuous line just about started spreads droplet its time 0.02 sec, similarly the continuous thin line shows after time 0.04 sec. figure 3.1.4 simulation results plot for film thickness with function of time.

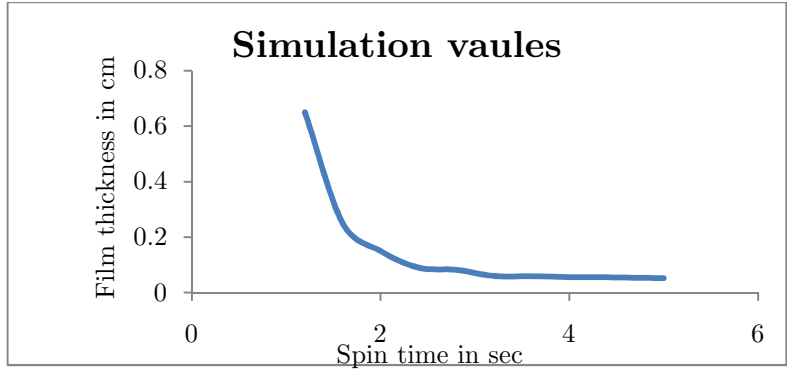


Fig 3.5 Film thickness when increasing time

3.2. Validation of results.

Previous section I had discussed about how the droplet spreading takes place on horizontal surface has function of time. Now the droplet fully spreads on the surface of disc, am comparing the simulation results with theoretical result.

From the theoretical point of view initial volume of droplet is equal to final volume of drop on disc surface.

$$\text{Volume of Droplet} = \frac{4\pi r^3}{3}$$

$$\text{Volume of fluid on Disc} = \pi R^2 h$$

$$\text{Film thickness } h = \frac{4}{3} \left[\frac{r}{R} \right]^2 r$$

Final film thickness from theoretical value is **5.33*E-2cm.**

Final film thickness from simulation is **5.2*E-2cm.**

Error 2.43 %.

Error 2.43 % because the droplet splashing (wasting) out from the horizontal disc. From this point view mesh working well, so I can implement same mesh for rotation of horizontal disc.

3.3 Droplet spreading on rotating disc

The relevant parameters in spin coating are the fluid properties: density ρ , viscosity μ and surface tension γ and the process parameters dosing volume V_0 , rotation speed ω , the liquid height h , liquid radius R , and the elapsed time t .

Final thickness formula

$$h = \frac{h_0}{\left(1 + \frac{4 \rho \omega^2}{3 \eta} h_0^2 t\right)^{\frac{1}{2}}},$$

Previous section discussed about when the horizontal is stationary and how the droplet spreading take place, and cause of gravity and surface tension only its completely spreading takes place. That is very limited applications, where the small applications can be used.

Now the horizontal disc is rotated, initial droplet will spreads on horizontal disc and start rotate to certain rpm which will cause film thickness will go very thin. Mainly due to centrifugal force which is acting out ward direction from the disc due rotation. However viscous force acting offsite of centrifugal force.

The droplet spreading takes place depending on fluid properties like viscosity, density and surface tension. Other properties like temperature of disc, disc rpm substrate surface.

Different fluids have a different viscosity when more viscosity of fluid spreading takes place more time and thickness will be high, when viscosity is less spreading will fast and very thin films we can get.

Depending on the disc speed and spin time film thickness can be varied. Previous sections were the validation now the mesh is working well next simulation for different viscosity of fluid.

3.4 Droplet spreading on rotation disc for different viscosity

First case where the disc rotating with constant speed and varying the viscosity of fluid, in this thesis I had taken four viscosity values like 0.001, 0.01, 0.1, 1 kg/m s below table show the theoretical value of each viscosity

Time in sec	Film thickness in cm V=0.001kg/ms	Film thickness in cm V= 0.01 kg/m s	Film thickness in cm V= 0.1 kg/m s	Film thickness in cm V= 1 kg/m s
2	5.76E-02	1.55E-01	2.52E-01	2.76E-01
4	4.11E-02	1.19E-01	2.32E-01	2.73E-01
6	3.37E-02	1.00E-01	2.16E-01	2.70E-01
8	2.92E-02	8.83E-02	2.01E-01	2.68E-01
10	2.62E-02	7.98E-02	1.91E-01	2.65E-01
12	2.39E-02	7.33E-02	1.82E-01	2.62E-01
14	2.21E-02	6.82E-02	1.74E-01	2.60E-01
16	2.07E-02	6.40E-02	1.67E-01	2.57E-01
18	1.95E-02	6.05E-02	1.60E-01	2.55E-01
20	1.85E-02	5.76E-02	1.55E-01	2.52E-01
22	1.77E-02	5.56E-02	1.49E-01	2.50E-01
24	1.69E-02	5.27E-02	1.45E-01	2.48E-01
26	1.63E-02	5.07E-02	1.41E-01	2.46E-01
28	1.57E-02	4.89E-02	1.37E-01	2.44E-01
30	1.51E-02	4.73E-02	1.33E-01	2.41E-01

Table 3.2 results of theoretical value for a different viscosity

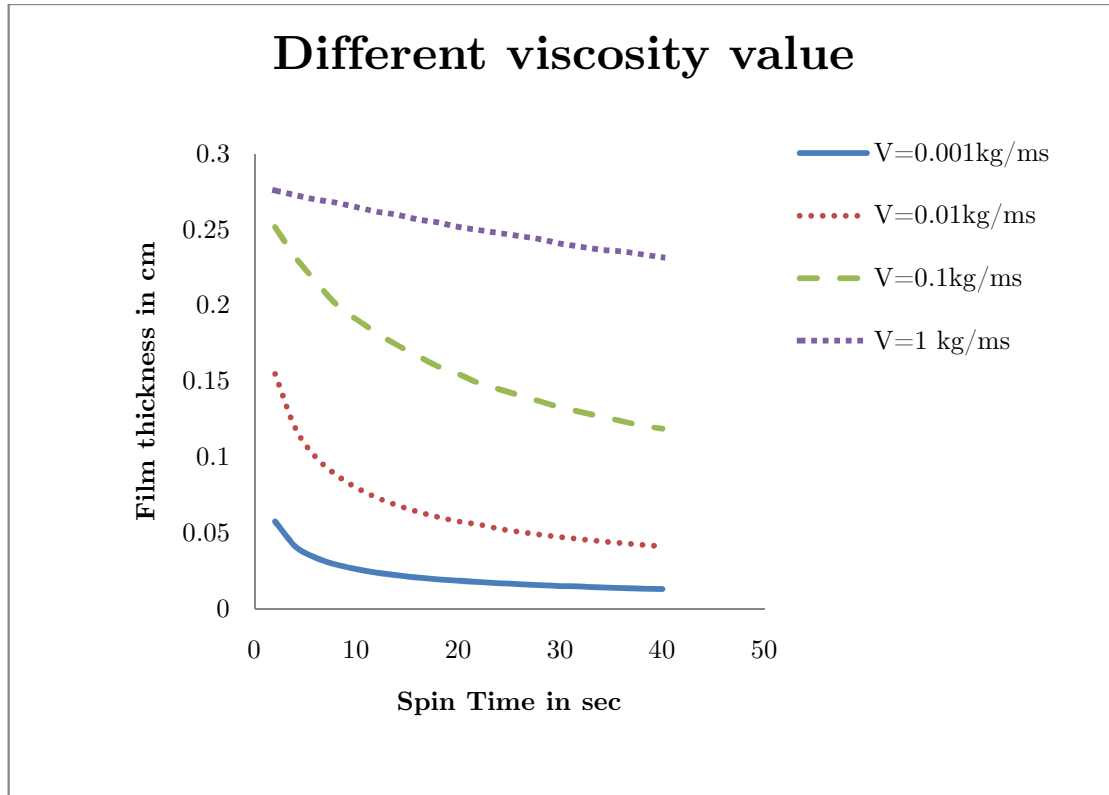


Fig 3.6

Fig 3.6 Theoretical film thickness for different viscosity

All parameter are same has the stationary horizontal surface simulation but addition parameter called disc speed.

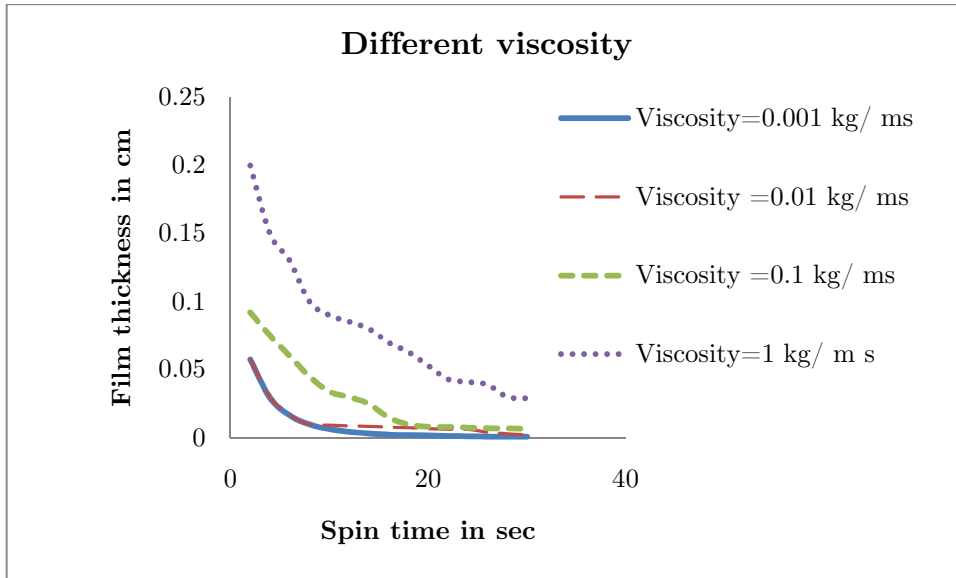
Above graphs show (3.6) the different viscosity of fluid film thickness which is theoretically formulated.

Viscosity of 0.001 kg/ms which is continuous line in graph when increasing spinning time film thickness goes on decreases due the fluid fallout by long spin or excess amount of fluid can be removed by spinning more time. When increases more spin time somewhere film thickness will be going to remain constant because fluid thickness will stick with the substrate and also can be treated fluid can't come out from the viscose force, viscose force dominate more than the centrifugal force.

3.5 Simulation results for different viscosity

Time in sec	Film thickness in cm V=0.001kg/ms	Film thickness in cm V= 0.01 kg/m s	Film thickness in cm V= 0.1 kg/m s	Film thickness in cm V= 1 kg/m s
2	5.76E-02	5.75E-02	9.20E-02	2.00E-01
4	2.95E-02	3.00E-02	7.50E-02	1.50E-01
6	1.65E-02	1.70E-02	6.00E-02	1.30E-01
8	9.90E-03	1.00E-02	4.50E-02	1.00E-01
10	6.50E-03	9.50E-03	3.40E-02	9.00E-02
12	4.55E-03	9.00E-03	3.00E-02	8.53E-02
14	3.33E-03	8.50E-03	2.50E-02	8.00E-02
16	2.45E-03	8.00E-03	1.50E-02	7.00E-02
18	2.10E-03	7.50E-03	9.90E-03	6.30E-02
20	1.80E-03	7.00E-03	8.20E-03	5.30E-02
22	1.45E-03	6.50E-03	8.00E-03	4.30E-02
24	1.25E-03	6.40E-03	7.50E-03	4.10E-02
26	1.02E-03	4.30E-03	7.13E-03	3.90E-02
28	1.00E-03	3.10E-03	7.00E-03	3.00E-02
30	9.50E-04	2.20E-03	6.80E-03	2.90E-02

Table 3.3 simulation results for different viscosity



(a)

Figure 3.7.1 Simulation results for different viscosity

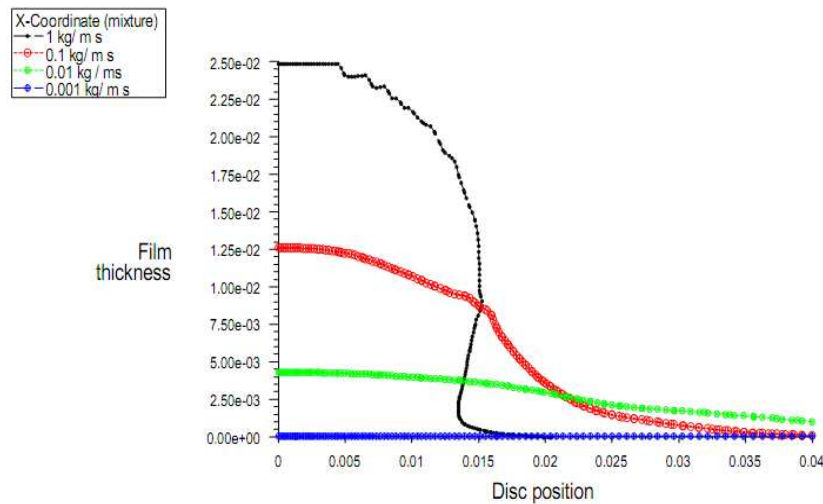


Fig 3.7.2 for constant time film thickness for different viscosity

Figure 3.7.2 shows the 0.03 sec of spin time high viscosity droplet continuous dotted and small width line spreading very slowly; film thickness of fluid is high shown Fig 3.7.2 0.025cm at the exactly middle of the disc. Continuous and more width line shows the viscosity of fluid is less compare to high viscosity fluid line at exactly middle of disc shown in Fig 3.7.2. We

can clearly see Fig 3.7.2 the very high viscosity of fluid about spread but the low viscosity of fluid spreads already on the horizontal disc. The main factor affecting thickness is viscosity, when more viscosity droplet spreading is less compare to low viscosity.

Comparing the simulation results with theoretical results

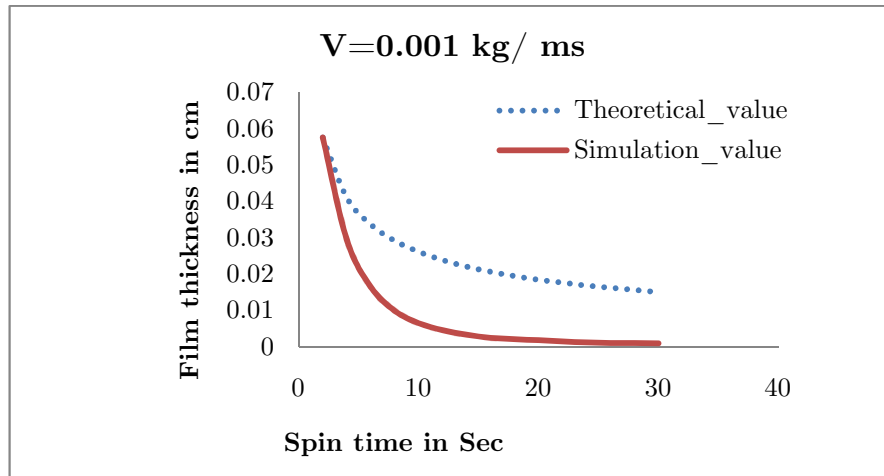


Figure 3.8 comparing the simulation results with theoretical results

Figure 3.8 shows the compare between the theoretical and simulation value, previous section 3.1 formulation of film thickness from theoretically, simulation thickness of graph for the same viscosity shown in figure 3.8 when increases in spin time and decreasing the film thickness, both are decreasing but there is error between theoretical value and simulation value due to mass transfer.

3.6 Droplet spreading on rotation disc with different rpm

Previous section discussed disc rpm is constant; here the droplet is spreading with a different rpm.

Theoretical results for different rpm

Time in sec	Film thickness in cm For 60 rpm	Film thickness in cm For 60 rpm	Film thickness in cm For 60 rpm	Film thickness in cm For 60 rpm
0.2	3.06E-02	2.05E-02	1.52E-02	1.23E-02
0.4	2.17E-02	1.45E-02	1.08E-02	8.71E-03
0.6	1.77E-02	1.18E-02	8.89E-03	7.11E-03
0.8	1.53E-02	1.02E-02	7.70E-03	6.16E-03
1.0	1.37E-02	9.18E-03	6.89E-03	5.51E-03
1.2	1.25E-02	8.38E-03	6.29E-03	5.03E-03
1.4	1.16E-02	7.76E-03	5.82E-03	4.66E-03
1.6	1.09E-02	7.26E-03	5.45E-03	4.36E-03
1.8	1.02E-02	6.85E-03	5.13E-03	4.11E-03
2.0	9.74E-03	6.49E-03	4.87E-03	3.90E-03
2.2	9.29E-03	6.19E-03	4.64E-03	3.71E-03
2.4	8.89E-03	5.93E-03	4.45E-03	3.56E-03
2.6	8.54E-03	5.70E-03	4.27E-03	3.42E-03
2.8	8.23E-03	5.49E-03	4.12E-03	3.29E-03
3.0	7.95E-03	5.30E-03	3.98E-03	3.18E-03

Table 3.4 Theoretical results for different disc rpm.

Simulation results for different rpm

Time in sec	Film thickness in cm For 60 rpm	Film thickness in cm For 90 rpm	Film thickness in cm For 120 rpm	Film thickness in cm For 150rpm
0.2	2.00E-02	1.90E-02	1.42E-02	1.00E-02
0.4	1.80E-02	1.30E-02	9.00E-03	7.71E-03
0.6	1.50E-02	1.10E-02	8.00E-03	6.21E-03
0.8	1.30E-02	9.00E-03	7.00E-03	5.16E-03
1.0	1.20E-02	8.00E-03	5.00E-03	4.50E-03
1.2	1.10E-02	7.40E-03	4.00E-03	3.90E-03
1.4	9.70E-03	7.00E-03	3.80E-03	3.50E-03
1.6	9.00E-03	6.00E-03	3.50E-03	3.00E-03
1.8	8.00E-03	5.20E-03	3.00E-03	2.70E-03
2.0	7.40E-03	5.00E-03	2.50E-03	2.30E-03
2.2	7.00E-03	4.50E-03	2.70E-03	2.00E-03
2.4	6.50E-03	3.90E-03	2.30E-03	1.90E-03
2.6	6.00E-03	3.00E-03	2.00E-03	1.80E-03
2.8	5.50E-03	2.00E-03	1.90E-03	1.70E-03
3.0	5.40E-03	1.20E-03	1.50E-03	1.30E-03

Table 3.5 Simulation results for different disc rpm.

Different rpm

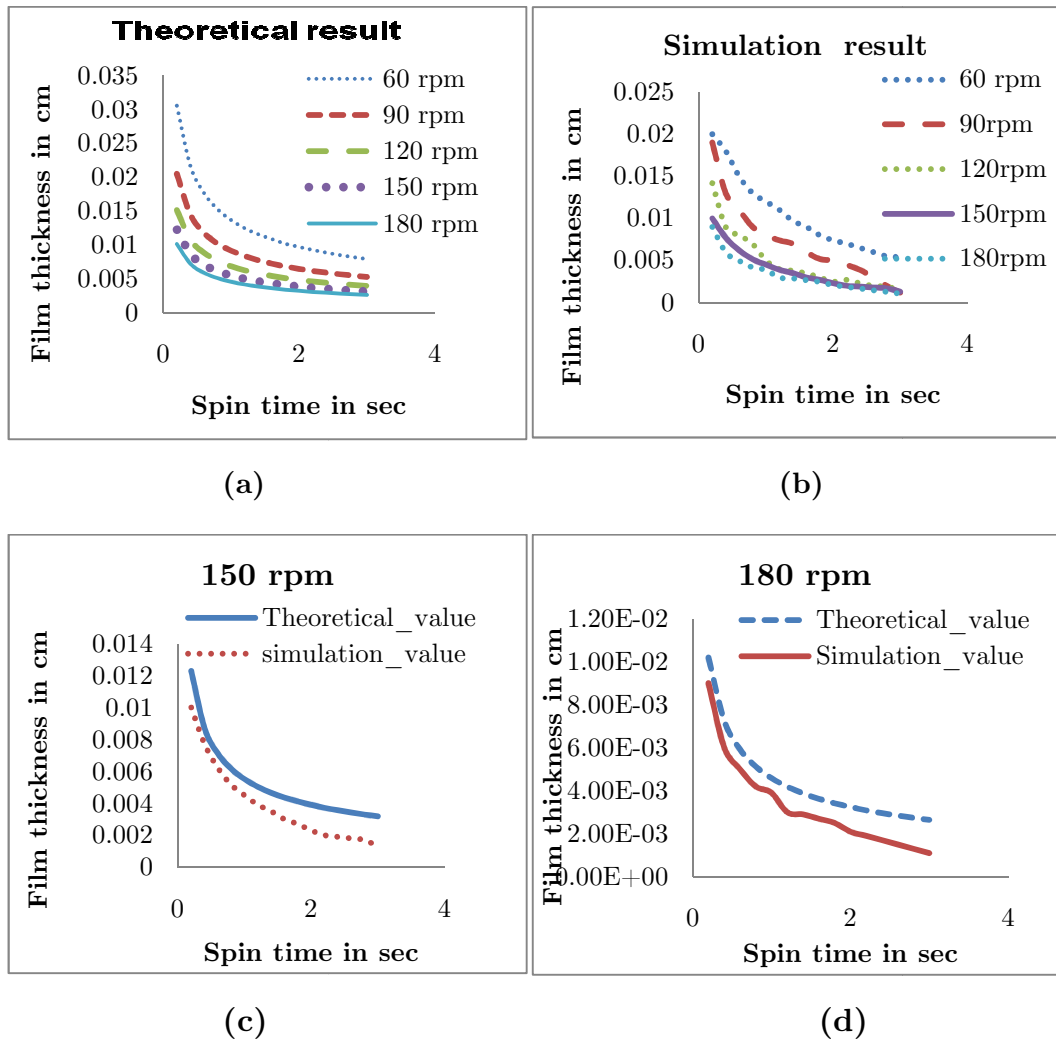


Figure 3.9 shows the theoretical and simulation results for different rpm

Figure (a) shows the theoretical film thickness for different rpm, when increase the rpm of the disc film thickness will goes on decreases. Figure 3.9 (b) shows the simulation film thickness for different rpm, both theoretical and simulation shows the same character of graph when increase the time of spin disc the film thickness decrease, for the disc of more rpm film thickness is less compare to less rpm at the spin of same time. Figure 3.9 (c) and (d) shows the difference of simulation and theoretical results, for 150 rpm and 180 rpm. Theoretical results indicated continuous line shown figure (c) and simulation results indicated dotted line in the same.

3.7 Droplet spreading on rotating considering the thermo effect (temperature depended viscosity) and thermo capillarity (temperature depended surface tension).

When heating the disc at certain temperature there will be thermo effect, viscosity of the fluid depending on temperature equation 2.9 and thermo capillary action equation 2.10. Previous section was discussed droplet spreading on disc considered all the parameter at room temperature, this section droplet spreading on disc by considering the both thermo effect and thermo capillarity.

Here considering both temperature dependent viscosity and temperature dependent surface tension, figure 3.10 shows the center of disc film thickness of $7E-3$ of normal temperature and $4E-3$ of temperature of $350k$. Droplet spreading faster rate where the temperature of disc is $350k$ compare to $300k$ temperature has show figure 3.10.

Two temperatures 300k and 350k compare at disc speed of 100 rpm

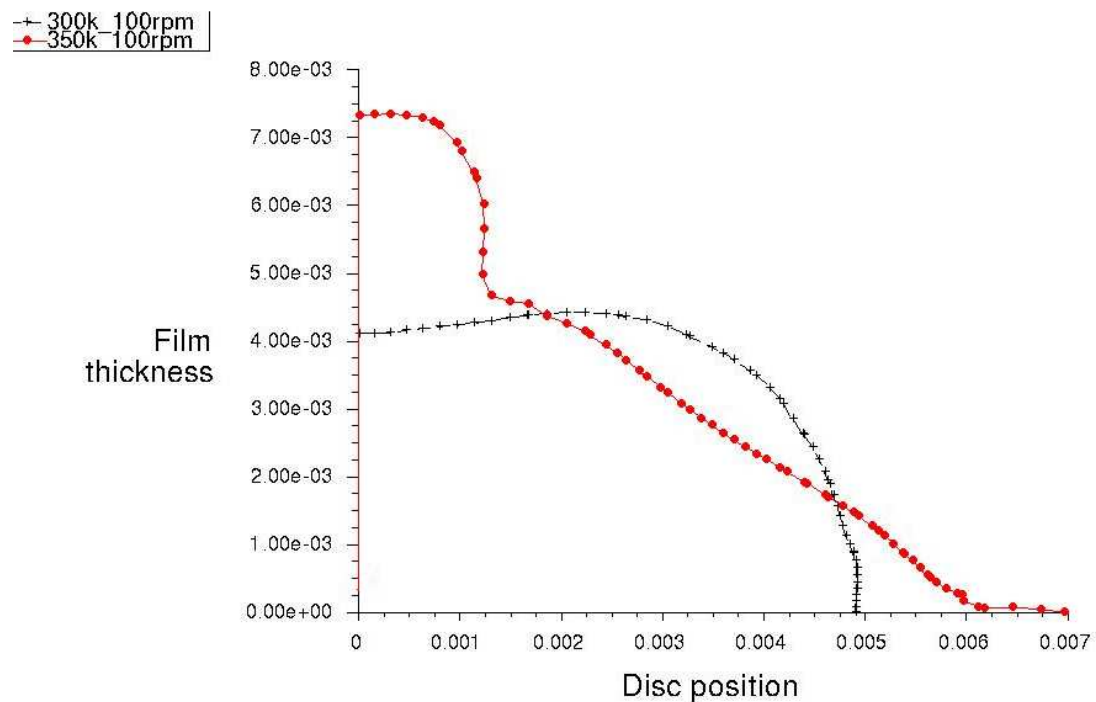


Figure 3.10 for constant disc rpm and spin time with varying the temperature of the disc

Disc temperature 350k for different rpm of disc

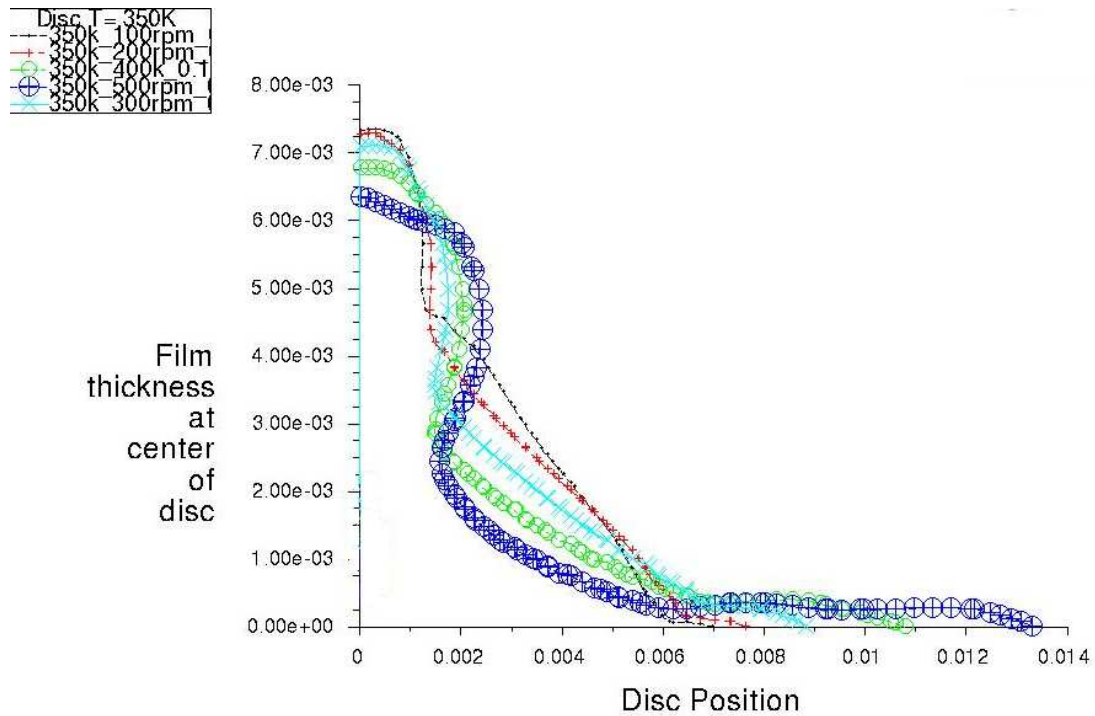


Figure 3.11 for constant temperature and spin time with varying the different disc rpm

Previous section 4.2 was discussed for different viscosity of fluid, when decreasing the viscosity of fluid droplet spreading fast and will get thin film compare to more viscosity of fluid. Section 4.2.3 was had discussed about for different of the disc, when increasing the rpm film thickness will goes on decreases. Here will be focus on droplet spreading on disc when increasing disc temperature of 350k fluid will for a different temperature and spinning disc (rpm). Figure 4.4.1 shows the for a constant disc temperature (350K) with different rpm.

Room temperature 303 k		Temperature 450 k		Temperature 500	
Disc rpm	Film thickness in cm	Disc rpm	Film Thickness in cm	Disc rpm	Film Thickness in cm
120	9.0E-3	120	2.3E-3	120	1.9E-3
150	7.7E-3	150	2.1E-3	150	1.0E-3
180	6.0E-3	180	1.2E-3	180	9.8E-4

Table 3.6 film thickness for different temperature and disc rpm

For 120 rpm

The difference of thickness when increasing the temperature of disc and compare 450k

$$9.0E-3 - 2.3E-3 = \mathbf{6.7E-3 \text{ cm}}$$

With 500k

$$9.0E-3 - 1.9E-3 = \mathbf{7.1E-3 \text{ cm}}$$

450k and 500k

$$2.3E-3 - 1.9E-3 = \mathbf{0.4E-3 \text{ cm}}$$

when large temperature difference of disc 303k and 450 k decrease thickness will be more (6.7E-3), for the same speed 450k to 500k temperature difference less is (0.4E03).

Advantage of spin coating

1. Spin coating has many advantages in coating operations with its biggest advantage being the absence of coupled process variables.
2. Film thickness is easily changed by changing spin speed, or switching to a different viscosity photo resist. But among the alternative coating techniques, many have multiple coupled parameters, making coating control more complex.
3. Another advantage of spin coating is the ability of the film to get progressively more uniform as it thins, and if the film ever becomes

completely uniform during the coating process, it will remain so for the duration of the process

4. It is low cost and fast operating system.

Disadvantages of spin coating process

1. The disadvantages of spin coating are few, but they are becoming more important as substrate sizes increase and photoresist costs rise.
2. First of all, as substrate sizes get larger, the throughput of the spin coating process decreases. Large substrates cannot be spun at a sufficiently high rate in order to allow the film to thin and dry in a timely manner resulting in decreased throughput.
3. The biggest disadvantage of spin coating is its lack of material efficiency. Typical spin coating processes utilize only 2-5 % of the material dispensed onto the substrate, while the remaining 95-98 % is flung off into the coating bowl and disposed.
4. Not only are the prices of the raw photoresist increasing substantially, but disposal costs are increasing as well

Conclusion

- We have successfully shown simulation spin coating, uniform thin film of water on horizontal disc.
- Simulation results match with against theoretical results, for different parameter effecting.
- Allowing the prediction of film thickness based upon key operating parameters such rotational speed, temperature of disc and fluid properties like density, viscosity and surface tension.
- Promises many benefits, and opens the way for the use of spin coating process.

Appendix

Now take cylindrical polar coordinates $(\mathbf{r}, \boldsymbol{\theta}, \mathbf{z})$ rotating with the spinning disk at angular velocity $\boldsymbol{\nu}_R$. The z dependence of the radial velocity $\boldsymbol{\nu}_R$ of the liquid at any point $(\mathbf{r}, \boldsymbol{\theta}, \mathbf{z})$ can be found by balancing the viscous and the centrifugal forces per unit volume, the centrifugal force working in the radial direction and the viscous shear stress in the opposite direction.

$$-\eta \frac{\partial^2 v_R}{\partial z^2} = \rho \omega^2 r \quad (2.5)$$

Equation can be integrated employing the boundary conditions that $\boldsymbol{\nu}=0$ at the surface of the disk ($z=0$) and that $\frac{\partial v}{\partial z} = 0$ at the free surface of the liquid ($z=h$) where the shearing force must vanish. Thus

$$v_R = \frac{1}{\eta} \left(-\frac{1}{2} \rho \omega^2 r z^2 + \rho \omega^2 r h z \right) \quad (2.5.1)$$

The radial flow q per unit length of circumference is

$$q = \int_0^h v_R dz = \frac{\rho \omega^2 r h^3}{3\eta} \quad (2.5.2)$$

To obtain a differential equation for h the equation of continuity is applied, reduction of height must balance with the radial flux,

$$\frac{\partial h}{\partial t} = -\frac{1}{r} \frac{\partial (rq)}{\partial r} = -\frac{\rho \omega^2}{3\eta} \frac{1}{r} \frac{\partial}{\partial r} (r^2 h^3) \quad (2.5.3)$$

Instead of solving this equation we can consider the fact that this equation has a special solution which only depends on t . In this case

$$\frac{\partial h}{\partial t} = -2 \frac{\rho \omega^2}{3\eta} h^3 \quad (2.5.4)$$

and this can be solved, defining $h(t=0)=h_0$ as the initial height of the fluid,

$$\text{Film thickness } h = \frac{h_0}{\left(1 + \frac{4\rho\omega^2}{3\eta} h_0^2 t\right)^{1/2}}, \quad (2.6)$$

References

- [1] Dwight G. Weldon. Failure analysis of paints and coatings. John Wiley & Sons, Ltd. 2009.
- [2] R. Lupoi and W. O'Neill. Deposition of metallic coatings on polymer surfaces using cold spray. Volume 205, issue 7 (2009), pages 2167-2173.
- [3] Jürgen M. Lackner. Industrially-scaled large-area and high-rate tribological coating by Pulsed Laser Deposition. Volume 200, issues 5-6 (2005), pages 1439-1444.
- [4] H. Sirringhaus, P.J. Brown, R.H. Friend, Janssen, M.M. Nielsen, K. Bechgaard, B.M.W. Langeveld-Voss, A.J.H. Spiering, R.A.J. Janssen, E. W. Meijer, P. Herwig and D.M. de Leeuw. Two-dimensional charge transport in self-organized, high-mobility conjugated polymers. Nature 401 (2009), pages 685-688.
- [5] Tzung-Fang Guo and Yang Yang. In situ study on the reorientation of polymer chains in operating polymer diodes. Applied Physics letters volume 80 (2002).
- [6] Andrew Mills. Oxygen indicators and intelligent inks for packaging food. Chem. Soc. Rev., (2005), 34, pages 1003–1011.
- [7] W.P. Jakubik, M. Urbanczyk, E. Maciak and T. Pustelny. Polyaniline thin films as a toxic gas sensors in SAW system. Molecular and Quantum Acoustics vol. 28 (2007).
- [8] D. W. Xu, Soon Fatt Yoon, and C. Z. Tong. Self-Consistent Analysis of Carrier Confinement and Output Power in 1.3- μm InAs–GaAs Quantum-Dot VCSELs. IEEE Journal of quantum electronics, vol. 44, (2008).
- [9] R. Wilson, D.J. Schiffrin, B.J. Luff and J.S. Wilkinson. Optoelectrochemical sensor for lead based on electrochemically assisted solvent extraction. Sensors and Actuators B, (2000), 63, pages 115-121.

- [10] S. Walheim¹, E.Schaffer and U. Steiner. Self-organized organic nanostructures: structure formation in thin polymerblend films. *Surf. Interface Anal.* (2004), 36 pages 195–196.
- [11] Stéphane Fierro and Christos Comninellis. Kinetic study of formic acid oxidation on Ti/IrO₂ electrodes prepared using the spin coating deposition technique. Volume 55, Issue 23, 30 (2010), pages 70-73.
- [12] Piotr Jasinski, Sebastian Molina, Maria Gazda, Vladimir Petrovsky, Harlan U. Applications of spin coating of polymer precursor and slurry suspensions for Solid Oxide Fuel Cell fabrication. *Journal of Power Sources* 194 (2009) pages 10–15.
- [13] R. Wilson, D.J. Schiffrin, B.J. Luff and J.S. Wilkinson. Optoelectrochemical sensor for lead based on electrochemically assisted solvent extraction. *Sensors and Actuators B*, 2000, 63, pages 115-121.
- [14] Xiaohu Yan, Guojun Liu, Michael Dickey and C. Grant Willson Preparation of porous polymer membranes using nano- or micro-pillar arrays as templates. Volume 45, Issue 25(2005), pages 8469-8474.
- [15] S.N. Reznik, and A.L. Yarin. Spreading of an axisymmetric viscous drop due to gravity and capillarity on a dry horizontal wall. *International Journal of Multiphase Flow* 28 (2002) 1437–1457.
- [16] M. V. Bartashevich Vladimir, V Kuznetsov and Oleg A. Kabov . Gravity Effect on the Axisymmetric Drop Spreading. *Microgravity Sci. Technol* (2010) 22 pages 107–114.
- [17] Siddhartha F. Lunkad, Vivek V. Buwa and K.D.P. Nigam. Numerical simulations of drop impact and spreading on horizontal and inclined surfaces *Chemical Engineering Science* 62 (2007) pages 7214 – 7224.
- [18] Maxime Nicolas. Spreading of a drop of neutrally buoyant suspension. *J. Fluid Mech.* (2005), vol. 545, pp. 271–280.
- [19] Niranjana sahu, B parija and S panigrahi. Fundamental understanding and modeling of spin coating process: A review. *Indian J. Physics.* 83 (2009) pages 493-502.
- [20] YIH-O TU. Contact Line Slippage of Fluid Flow on a Rotating Disk”. Academic Press, Inc. IBM Almaden Research Center 1987.

- [21] P.Yimsiri, M.R. Mackley. Spin and dip coating of light-emitting polymer solutions: Matching experiment with modeling. *Chemical Engineering Science* 61 (2006) pages 3496 – 3505.
- [22] P. Temple-Boyer, L. Mazenq, J.B. Doucet, V. Conédéra, B. and Torbiéro, J. Launay. Theoretical studies of the spin coating process for the deposition of polymer-based Maxwellian liquids. *Microelectronic Engineering* 87 (2010) pages 163–166.
- [23] Piotr Jasinski, Sebastian Molin, Maria Gazda, Vladimir Petrovsky and Harlan U. Andersonc. Applications of spin coating of polymer precursor and slurry suspensions for Solid Oxide Fuel Cell fabrication. *Journal of Power Sources* 194 (2009) pages 10–15.
- [24] Lin Wu. Thermal effects on liquid film dynamics in spin coating. *Sensors and Actuators A* 134 (2007) pages 140–145.
- [25] Konstantin Vorotilov, Vladimir Petrovsky and Vladimir Vasiljev, Spin Coating Process of Sol-Gel Silicate Films Deposition: Effect of Spin Speed and Processing Temperature. *Journal of Sol-Gel Science and Technology*,(1995) pages 173-183.
- [26] Mizue munekata, Seiichi kimura , Hiroaki kurishima and Hideki Ohba. Effect of Catch Cup Geometry on 3D Boundary Layer Flow over the Wafer Surface in a Spin Coating. *Journal of Thermal Science* Vol.17, No.1 (2008) pages 56-60.
- [27] James Derksen, Sangjun Han and Jung-I-loon Chun. Extrusion-Spin Coating: An Efficient Photoresist Coating Process for Wafers. *Semiconductor Manufacturing Conference Proceedings, 1999 IEEE International Symposium on Issue* (1999), pages 245-248.
- [28] John M, Prausnitz, and John P O’connell. *The properties of gases and liquids*. Fifth edition Mc-Graw-hill 2001.
- [29] Jie Li, Yuriko Y. Renardy. Shear-induced rupturing of a viscous drop in a Bingham liquid. *J. Non-Newtonian Fluid Mech.* 95 (2000) pag235–251.
- [30] Akihiro Kitamura. Thermal effects on liquid film flow during spin coating. *Physics of fluids* volume 13, (2001).